



**Politecnico
di Torino**



Politecnico di Torino

Department of Mechanical and Aerospace Engineering

&

FPT powertrain Technologies

Department of P.E Control system and software-Mechatronic components

Master Thesis in Automotive Engineering

Academic Year 2022-2023

December 2023

Natural gas circuit design

Pressure loss analysis prediction model and simulation

Supervisors:

Prof. Baratta Mirko

Ing. Riesi Paolo

Candidate:

Karthik Sakthivel

S289672

ABSTRACT

The present work aims in:

- Modeling and simulating the heavy haul truck fuel line from vehicle tank to engine through filter, pressure regulator, fuel injection common rail and the injector of natural gas-powered (Compressed Natural Gas and Liquefied Natural Gas also said CNG and LNG)
- The calculation of their pressure loss in the fuel line from Vehicle tank to Engine

The model was developed in the GT SUITE software that enable the users to evaluate the pressure loss by faster 1D simulation. 1D simulation was opted to run and simulate different input tank pressures, engine load conditions, temperature variations, density of the fuel, fuel quality. The main contributors for the pressure loss are identified during the simulations. The case sweep was done for cross analysis and the results compared with the pressure, flow conditions, there-by suggested pipe dimensions with modified layout are given as output to improve the efficiency of engine performance and reduce the power lag during the transient operation condition.

The results from the simulation results were correlated and validated by the inputs from the Engine test bench

CONTENTS

ABSTRACT	5
1. INTRODUCTION.....	8
1.1 Sustainable goals under this thesis	8
1.1.1 SDG 11.....	8
1.1.2 SDG 12.....	8
1.1.3 SDG 13.....	8
1.1.4 SDG 8.....	8
1.2 About methane (CH ₄)	9
1.3 About natural gas properties	9
1.3.1 LNG properties.....	9
1.3.2 CNG Properties	9
1.4 Development towards 2030 (EU)	10
1.5 FPT Industrial S.p.A. company profile	14
1.5.1 About FPT Industrial S.p.A. Natural Gas Engine lineup: engineering for sustainability	14
1.6 CNG and LNG Layout	17
1.6.1 LNG vehicle layout	17
1.6.2 CNG vehicle layout.....	18
1.7 Details of main components	18
1.8 Problem statement.....	24
2. Laboratory test bench.....	25
2.1. Description	25
2.2. High Level Simulation	26
2.3. Deep Level Simulation	32
2.4. Layout optimization investigation.....	41
3. Vehicle simulation	49
3.1 Description	49
3.2 CNG high level vehicle simulation	49
3.3 CNG deep level vehicle simulation	54
3.4.2 Pressure loss analysis of different cross section	65
3.4 LNG high level vehicle simulation	69
3.5 LNG deep level Vehicle layout.....	71
3.5.1 LNG vehicle simulation deep level results:	73

Diameter Swap study.....	76
3.6.1 Vehicle simulation conclusions.....	81
3.7.1 Extension:	83
4.Conclusions	84
BIBLIOGRAPHY AND SOURCES	86

1. INTRODUCTION

1.1 Sustainable goals under this thesis



Fig. 1. 2 SDG 11



Fig. 1. 3 SDG 12



Fig. 1. 4 SDG 13

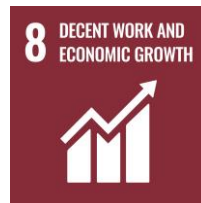


Fig. 1. 1 SDG 8

1.1.1 SDG 11

Sustainable cities and communities: The goal focuses on making cities and human settlements inclusive, safe, sustainable. It emphasizes to reduce environmental impacts of the cities and communities, enhance basic service for all people. Achieving this goal involves promoting affordable housing, **efficient public transportation**.

1.1.2 SDG 12

Responsible consumption and production: SDG12 aim to ensure sustainable consumption and production patterns. It promotes the need to do more with less, reducing waste and promoting sustainable practices across industries. Key elements include minimizing food waste, promoting **sustainable manufacturing and encouraging sustainable lifestyle such as promoting the sustainable fueled vehicles for the transportation fleet**.

1.1.3 SDG 13

This goal addresses the urgent need for **combat climate change** tipping point 1.5 C which is crucial for all life on Earth. It calls for stronger actions to reduce greenhouse gas emissions, enhance climate resilience and promote climate education and awareness. The development of bio-based fuel, near to zero emissions in the trucks (WTW) are developed for the new era of transportation which address the SDG 13

1.1.4 SDG 8

Decent work and Economic growth: SDG 8 promote the sustained, inclusive, and sustainable economic growth, employment, decent work for all. It emphasizes the importance of job creation, improving labor rights and fostering entrepreneurship. It also underscores the need to address the issues such as youth unemployment and labor market inequalities. The development of new technologies requires advanced education in new technologies, which involves job market for more young people, formation, and collaboration with new companies due to new technologies to sustain the SDG targets promoting more employment.

1.2 About methane (CH₄)

Methane is a chemical compound with the chemical formula CH₄ (one carbon atom bonded to four hydrogen atoms). It is a group-14 hydride, the simplest alkane, and the main constituent of natural gas. The relative abundance of methane on Earth makes it an economically attractive fuel, although capturing and storing it poses technical challenges due to its gaseous state under normal conditions for temperature and pressure.

Naturally occurring methane is found both below ground and under the seafloor and is formed by both geological and biological processes. Methane can be used as fuel on engine for automotive sector present into two different types: Liquified Natural Gas (L.N.G.) and Compressed Natural Gas (C.N.G.).

Methane is lighter than air, colorless and odorless gas which occurs in the nature abundantly as a product of agricultural and other human activities. It is a member of paraffin series of hydrocarbons and most potent of the greenhouse gases. The natural gas was composed 97 % of methane by volume and the rest was composed of Ethane 0.919% (C₂H₆), Propane 0.363% (C₃H₈), Butane 0.162% (C₄H₁₀), Carbon di oxide 0.527% (CO₂), Oxygen 0.08% (O₂), Nitrogen 0.936 (N₂) and other Noble gases (Helium, Neon, Argon, Xenon)

The methane gas is stored in the vehicle fuel tanks in compressed form at high pressure as CNG and in liquified form (LNG)

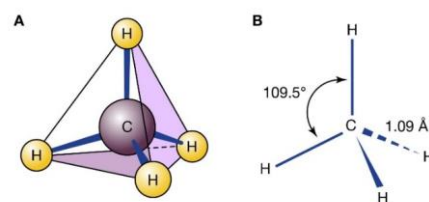
1.3 About natural gas properties

1.3.1 LNG properties

The natural gas was cooled to minus 160 C (minus 260 F) at atmosphere pressure and reduced to the liquid state which is 1:600 ratio to its original volume. LNG is colorless and odorless which is nontoxic and non-corrosive in nature. Due to cryogenic nature, LNG has the tendency to freeze ant material it contacts; thus, the evaporator was added in the vehicle system to heat up the fuel to gaseous form to be supplied to the engine. As a liquid LNG cannot explode and nonflammable.

1.3.2 CNG Properties

From the analysis, there are various factors which influence the gas composition such as geographical source of natural gas, source of origin, extraction date, production and refining process in the plant, transportation changes. These factors have influence in heating value, in methane number, stoichiometric air-fuel ratio and octane index. Sometimes there are hazardous components which affects the engines and components are the moisture content, oil and dust which are the parts which are contributors as a product of compressors used in the stations. As per the legislation standards ISO 15403:2006 defines that natural gas as a gas with more than 70% volume/mole of methane and higher calorific value of 30-45 MJ/Nm³, it also recommends



© Encyclopædia Britannica, Inc.

Fig. 1. 5 Methane bonding (source: Britannica inc)

limits for moisture and dust, 3 % volume for both G20 and G25 grade, less than 5mg/m³ for CO₂, O₂ and H₂S limit.

Different methane grades are possible based its purity. Generally, design must be done considering G20 and G25. The properties of G20 grade methane and biomethane, especially in the liquified form (LNG), is nearest to the pure methane. See following table as reference. G25 is containing 14% of nitrogen.

Composition		Test reference Gas			
		G20	G23	G25	Gr
Methane C1	%mol	99.5 ±0.5	92.5 ±1	86±2	87±2
Ethane C2	%mol	-	-	-	13±2
Balance	%mol Max	1	1	1	1
N2	%mol	-	7.5±1	14±2	-
S	Mg/kg Max	10	10	10	10
W.I.*	Nr (LHV)	48±0.2	44±0.5	41.5±1	48.5±0.5
MN	Nr	95 – 100	82 – 85	70 – 76	70 – 75
MON	Nr	137 – 140	128 – 130	120 – 124	120 - 126

Table 1. 1 Methane grade composition comparison

*Note: W.I. is Wobbe index indicating: the characteristic of gaseous fuels. The Wobbe index relates the heating characteristics of blended fuel gases. The Wobbe Index, which is a measure of the energy content of methane-based fuels, is derived from the fuel energy flow rate through a fixed orifice under given conditions. Mathematically, it is calculated using the heating value of the fuel and the square root of the fuel specific gravity. When calculated using the gross (higher) heating value of the fuel, it is called the Gross Wobbe Index. WI is important for vehicle/engine operation because it correlates directly with the indicated power output available from an engine.

Based on the study¹, there are several trace components must be closely controlled when using biomethane, CNG, LNG as a vehicle fuel including:

- Siloxanes (risk of abrasion and increased probability for knocking)
- Hydrogen (risk of Embrittlement for the metallic materials)
- Water, moisture content (risk of corrosion and drivability problems)
- Hydrogen sulfide, H₂S (corrosive in the presence of water could form acid and affect the after-treatment systems, combustion products could create problems by sticking engine valves, critical parts such as injection nozzles)

1.4 Development towards 2030 (EU)

A stronger focus in CO₂ emission reduction technologies is more and more required to reach the climate goals in 2030 and beyond. The current development of technologies that can contribute to CO₂ reduction in hydro fuel carbon road transports include the alternative fuels. Alternative fuels, e.g., natural gas for internal combustion engines can provide an intermediate and immediate solution with current production technologies unless minor changes in the layout and components to match with the emission regulations. Natural gas is considered one of the most eco-friendly fuels for internal combustion engines. It improves air quality significantly, reducing

¹ https://www.iea-amf.org/content/fuel_information/methane

pollutants; it mitigates global warming by significantly reducing CO₂ and other greenhouse gas emissions, and it also lowers acoustic pollution by reducing engine noise: a bio-gas-powered vehicle eliminates emissions while providing incredibly effective noise reduction.

For these reasons, Natural Gas long-haul trucks are being produced for the last couple of years by OEM like IVECO, SCANIA and VOLVO registering more market penetration.

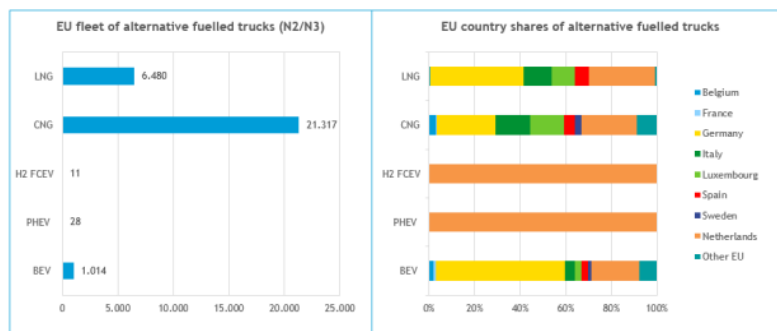


Fig. 1. 6 EU alternatively fueled truck fleet: totals and shares per country 2020 (source: Alternative Fuels observatory)

As consequence, also wider infrastructure footprint of public station in EU has been registered in the last years. The number of CNG and LNG stations increased

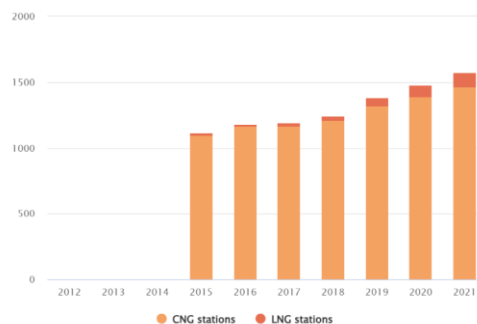


Fig. 1. 7 Number of CNG and LNG refueling points for trucks N2 and N3 in Italy(source: Alternative Fuels observatory)

Despite LNG and CNG trucks are estimated to be 30% more expensive in purchasing price, extra-price can be earned back due to the lower fuel costs. For this reason, natural gas vehicle is estimated to be current best possible solution for sustainable mobility compared to electric and fuel cells vehicle which still required better technology competitiveness and more infrastructure investments. Furthermore, the cost of ownership of BEV (Battery Electrical Vehicle) and FCET (Fuel Cell Electric Truck) vehicle is comparatively higher than the current natural gas technologies.

Furthermore, in the last years the capability to produce biofuel like bio-LNG by organic waste flows thanks and biomethane from organic matters has been increased thanks to incremental change of the driven technology. Even if current well to wheel efficiency is low, pilot production

plants such as SUNFIRE is scaling up in Germany and Norway making E-Fuels more of a limited option for the future. Thus, rapid expansion of biofuel is foreseen

	MJ/km	WTW g CO ₂ -eq/MJ	WTW CO ₂ -eq/km	
Diesel	11.1	95	1,051	
LPG	12.0	74	886	
CNG	10.5	69	728	
LNG	10.5	75	783	
FCEV-PEM (H ₂ -gas)	9.2	105	964	
FCEV-PEM (H ₂ -average electricity)	9.2	205	1,880	
BEV (electricity-average mix)	6.1	133	811	
Biodiesel (FAME, HVO)	11,1	14	149	
Bio-CNG	10.5	24	252	
Bio-LNG	10,5	29	307	
FCEV-PEM (H ₂ -wind energy)	9.2	6	54	
BEV (electricity-wind enery)	6.1	4	23	

Table 1. 2 Well to wheel emissions of truck trailer (GVW 40 ton) with different fuels and drivelines (MJ/km based on NEA 2019, JRC 2014 for H2 and CE delft 2020 for electricity; FCEV: Fuel Cell Electric Vehicle)

Bio-LNG production is expected to be 30% to 40% of EU total gas consumption by 2025 according to EBA (European Biogas Association). The need for bio-LNG in the transport sector is visible in bio-LNG production capacity (TWh/year) forecasts: in Europe it is expanding rapidly from 2018 to 2024 and could fuel almost 25000 LNG trucks for whole year as per EBA statistical report. The trend was given as follow.

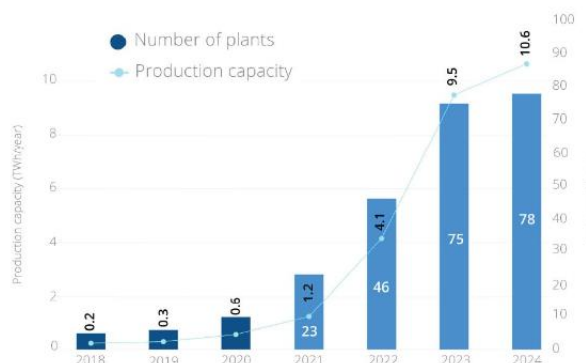


Fig. 1. 8 Production capacity (TWh/year) vs Number of plants in production capacity in Europe from 2018 to 2024(source: Nordsol)

About biomethane, today EU production is around 3.6 bcm. €4.1billion investments are planned between 2023 and 2025, while further €12.5 billion will be predicted to be unlocked in 2026-2030. In the first analysis, investments are primarily located in France (€1.4 billion) and Italy (€1.1 billion) who were top contributors in EU as per European Bio-gas association investment outlook of June 2023.

We can observe from the following data the transition from Diesel to Alternative fuel was already increasing at rapid rate to adopt to new emission regulations.

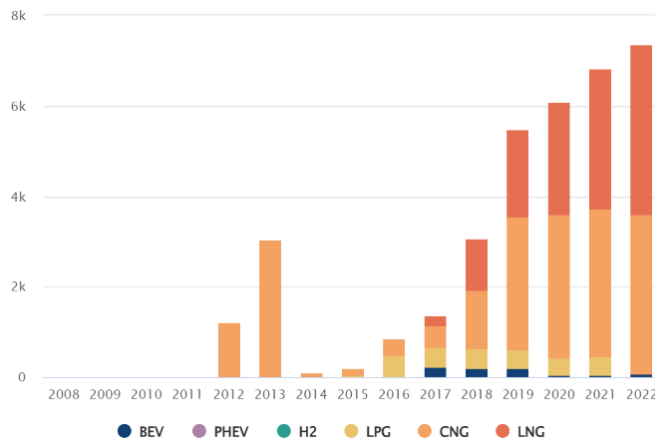


Fig. 1. 9 Total number of alternative fueled trucks fleet in Italy N2 & N3 (source: European Alternative Fuels Observatory)

1.5 FPT Industrial S.p.A. company profile

FPT industrial S.p.A. is an Italian brand of Iveco Group dedicated to design, produce and sale of powertrains and solutions for on-road and off-road vehicles, as well as marine, power generation applications. The company has around eleven production sites and eleven research and development centers around the world. The company's extensive product offers include the six engine ranges with power outputs from 42hp to over 1000hp, transmission with torque up to 500 Nm. FPT Industrial offers the most complete line-up of natural gas engines for industrial applications on the market, with power outputs ranging from 50 to 520 hp. A dedicated E-Powertrain division is accelerating the path towards net zero-emissions mobility, with electric drivelines, battery packs, and battery management systems.



Fig. 1. 11 FPT powertrain technologies logo



Fig. 1. 10 FPT natural gas engine featured in IVECO S-way truck(source: Iveco)

1.5.1 About FPT Industrial S.p.A. Natural Gas Engine lineup: engineering for sustainability

All FPT engine families include natural gas units to offer a reliable, advanced, clean engine designed for low noise and long life, everyday savings through low fuel and low carbon consumption, respecting the environment and current low emission restrictions. Whether they are on-highway engines for light, medium and heavy segment trucks, coaches, buses or special vehicles for emergency and defense: the result will be fuel-efficient performance and reliability. The current lineup for trucks application is capable to cover wide power range as reported below and has been recently updated with new XCUSOR 13 engines (also called xC13). The new xC13 is a breakthrough in this area and recognized as best-in-class performance making it a primary contributor to achieving the 2025 fleet-wide CO₂ emission targets where it is claimed with Bio methane it can reduce 95% CO₂ emissions. The xC13 is foreseen in production also for diesel and in future for hydrogen technology being ready for zero emission targets. The natural gas engine emits greatly reduced particulate matter, NO_x, and CO₂ at levels far below the current WLTP based targets in g CO₂/km in the upcoming 2025 to 2029 emission target range. The xC13 is evolution. from current CURSOR 13 NG and here below summary comparison is reported.





NEF Family		CURSOR Family	
N67 NG	CUSOR 9 NG	CUSOR 13 NG	XCUSOR 13 NG
162 – 210 kW	221 – 294 kW	338 kW	353 – 382 kW
			

Table 1. 3 Engine series of NEF and Cursor family

For the thesis purpose, the Engine with the similar architecture was considered with the two different form of methane used CNG and LNG which are used in the same engine series, even though they share same architecture and same fuel, since the form of storage of the methane plays different characteristics in the performance of the Engine, this is due to the different components which are used in the fuel line of Natural gas architecture of the vehicle. The difference in the engine performance and characteristics of engine Xc13 series are reported below:

	CURSOR 13 NG	XCURSOR 13 NG
Certification	Euro VI E	Euro VI E
No. of cylinders/valves	Inline 6 / 4V	Inline 6 / 4V
Injection system	Multi Point Injection	Multi Point Injection
Turbocharger	WG	eWG
Displacement [l]	12.9	12.9
Bore x Stroke [mm]	135 x 150	135 x 150
Max power [kW] @ [rpm]	338 @1900	353 @1900
Max Torque [Nm] @ [rpm]	2000 @ 1100	2200 @ 1100
Dry weight [kg]	1150	1050
Dimensions LxWxH [mm]	1610X1027X1178	1365x1067x1167
ATS	3-way catalyst	EGR 3-way catalyst

Table 1. 4 Engine performance characteristics of C13NG and xC13NG

Pros of methane-based fuel:

- Reduced emissions and cost-effective solution than BEV
- No dosing requirements in after treatment systems
- Complex exhaust regeneration systems are neglected, simple 3-way catalyst configuration.
- Reduced maintenance
- Fleet Mode and ECO fleet to maximize the consumption efficiency.

The overall fuel architecture is split into two major areas: **high pressure** and **low pressure** regulated by intermediate pressure regulator. High pressure systems consist mostly of vehicle chassis installed components such as tank mainstream pressure regulators. Low pressure system consists of mostly engine components such as Fuel rail, Flexi pipe and gas injector downstream pressure regulator. See following picture as reference.

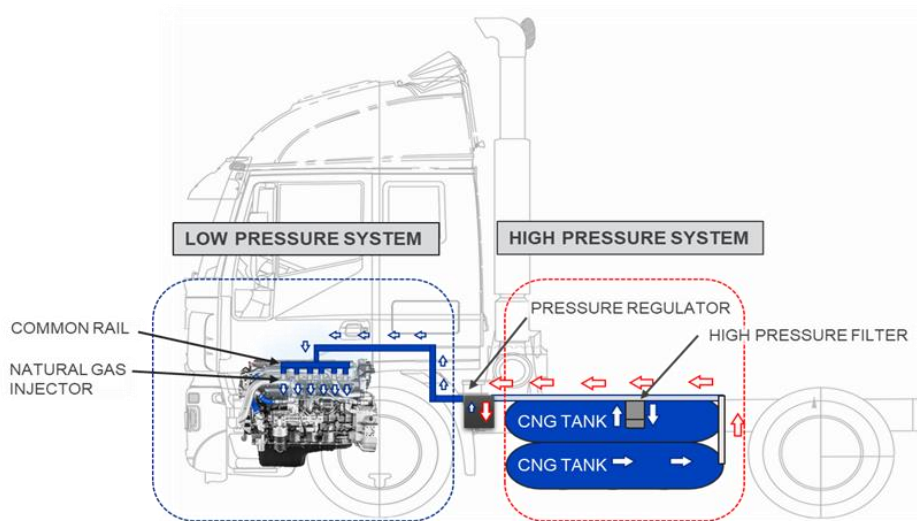


Fig. 1. 12 CNG system Layout (represents position of circuit from tank to Engine)

The gas flow starts from the CNG tank, which was at high pressure zone, which will be allowed to pass through the metallic tubes and reaches the Pressure regulator, the pressure regulator reduces the high-pressure gas into low pressure to supply the common rails and the injector where the pressure should be limited for the safe operation of the components also ensuring the minimum operating pressure ensuring the maximum flow of the gas. Then the gas will pass through the flexi pipe (metallic hose) which connects the common rail and the pressure regulator. Then the pipe is connected to the common rail, where it was attached to the intake manifold of the engine. The injector type used varies depending on the application.

1.6 CNG and LNG Layout

The scope of the study was conducted for the heavy duty (CURSOR series) engine applications used for on-road applications working with natural gas. The fuel into the vehicle can be stored in the compressed form (C.N.G.) or in liquid form (L.N.G.).

- Liquified methane (LNG, LBG): natural gas has been liquified after processing. The temperature is about -161.7°C at atmospheric pressure and it is stored in the on-board cryogenic tanks which will be vacuum isolated stainless-steel vessels, which have different operating pressure ranges.
- Compressed methane (CNG, CBG): natural gas or bio-methane has been compressed after processing which was used in automotive fuel and typically compressed up to 200 bar²

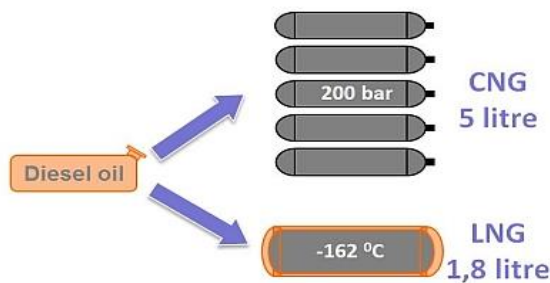


Fig. 1. 13 CNG/LNG and diesel energy and volume equivalence NGVA Europe

Vehicle can be equipped with only LNG (single or double LNG based on number of tanks), CNG only (with only one tank of CNG) and bi-fuel (in case of possibility to run either with CNG on one tank and LNG on another tank). See below vehicle layout and configuration of tanks for details.

1.6.1 LNG vehicle layout

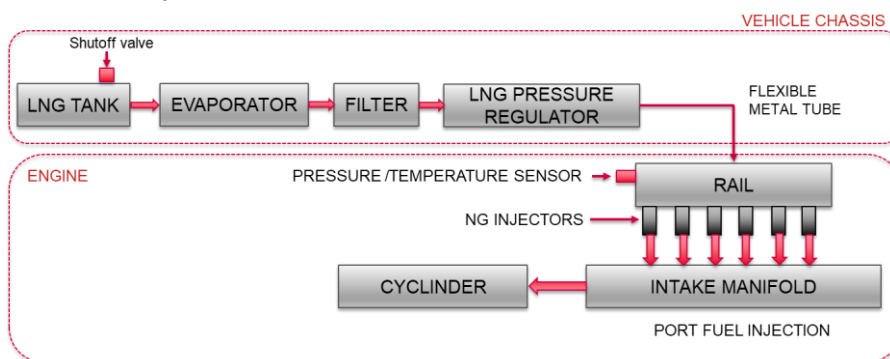


Fig. 1. 14 LNG layout representation from tank to intake manifold of the xC13 NG engine

The LNG vehicle layout contains the important components which includes the LNG tank which was a cryogenic tank with an evaporator inside the tank which vaporizes the liquified LNG into gaseous methane which then filtered by passing through the coalescence filter to separate the oils and moisture content if present. Pressure is regulated by the regulator to stabilize working pressure range. Downstream the regulator is the rail and six gas injectors which was attached at the end of the common rail injectors, here the port fuel injection is utilized, where the fuel and the atmospheric air was mixed in at stoichiometric proportion and feed into the cylinder for ignition, downstream the pressure regulator the process remains the same for LNG & CNG natural gas architecture.

1.6.2 CNG vehicle layout

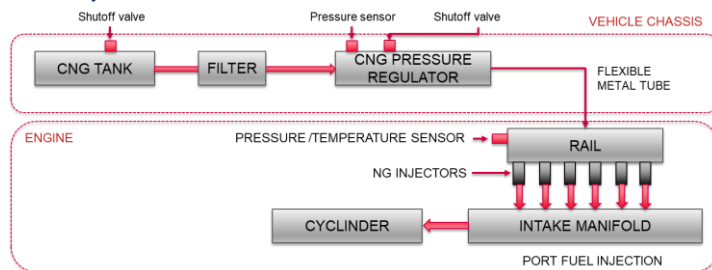


Fig. 1. 15 . CNG layout representation from tank to intake manifold of the xC13 NG engine

The CNG layout starts with the high-pressure storage tanks. The maximum capacity of the fuel depends on vehicle layout and space available on chassis. The shutoff valve ensures that the no gas leaks or allowed to pass through when the engine is turned off. The shutoff valve contains a solenoid valve which will be controlled via ECU signal, Gas is filtered by high pressure filter and then pressure regulator set the pressure to required optimal working pressure range in the common rail and the injectors. The shut off valve which was fixed in the pressure regulator ensures the closing of the valve when the engine is turned off. This act as a safety parameter in the CNG engine, ensuring no leakage occurs during the engine of condition. The pressure sensor in the pressure regulator measures the tank pressure and the pressure sensor and the temperature sensor present in the common rail was continuously feed to the ECU and the natural gas injectors are operated by the ECU depending on the engine load requirements.

1.7 Details of main components

1.7.1 CNG tank

In CNG tanks the natural gas was stored at highly compressed state where the pressure level reaches 200 barg when full and 20barg when tank pressure is minimum for optimum performance of the engine. The CNG operated vehicles has the range up to 1600 km and it differs based on the selection of the tank capacity and orientation in the layout. The layout configuration was shown below for reference.

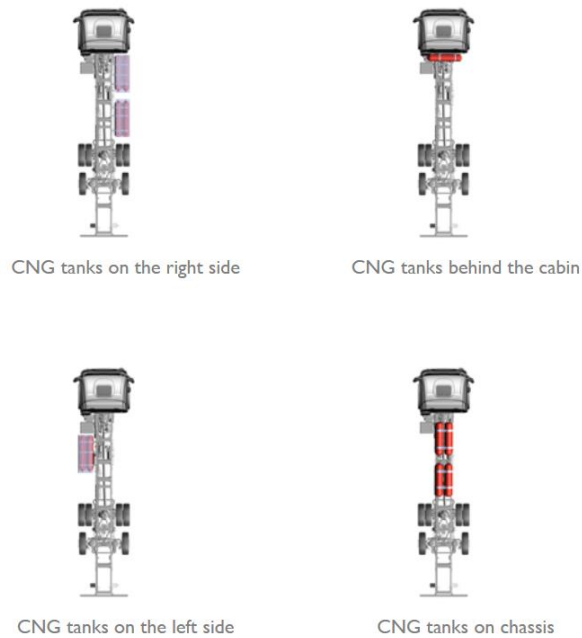


Fig. 1. 16 CNG tank configuration on vehicle layout

1.7.2 LNG tank

The LNG tanks can be opted in two range 540 liters and 410 liters, they can be used in different configurations. The maximum range of LNG with maximum capacity tanks can reach up to 1600 km of range without need for the refueling. The natural gas stored in the cryogenic temperature at -161.7°C at atmospheric temperature. The layout configuration was shown below for reference.



Fig. 1. 17 LNG tank configuration on vehicle layout

1.7.3 Coalescing Filter

The coalescence filter is a filtration system where it contains baffle screens or walls where the stream of fluid to be separated is applied to the filter, the baffles screen out the various particulate matters such as compressor oil, dust, impurities by trapping them in different sections, the oil gets collected at the bottom of the filter, where it can be drained at various intervals, this is important component in CNG since the gas when compressed at high pressure uses a compressor, the compressor during compression transfers the oil droplets to the storage tanks since it requires lubrication during compression, without coalescing filter, we will introduce the oil **particles to the engine , which has adverse effect on the engine and emission targets.**

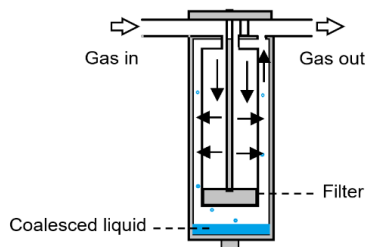


Fig. 1. 18 Coalescing filter

1.7.4 CNG pressure regulator

The CNG pressure in the storage tanks (max 260 barg) is being decreased down to the operating range of the fuel injection systems. The main components of pressure regulators are:

- Filter
- Shutoff valve
- Nozzles
- Cylinder Spring piston assembly
- Dynamic Sealing
- Pressure relief valve

The CNG pressure regulator functions by reducing the pressure in two stages, where initial pressure reduction was ranging 10-13.5 barg and the second stage reduces the pressure which keeps constant pressure which was set by the pressure regulator setpoint tuning screw, which was decided by factory setting, adjusting the screw after factory set limits lead to infringement of the component. The Coalescing filter was already built in the component downstream the first stage, followed by the second stage solenoid valve which was in closed position when the engine shutoff conditions. Following the second stage the boost assist was connected to the intake manifold to equalize the pressure. The heat exchanger is the crucial component in this CNG regulator since the high compressed gas when passed through the small orifice leads to high pressure difference which leads to high difference in temperature which leads to freezing of the component at low operating temperature (ambient), these are considered during the cold start conditions, since during the cold start, this heat exchanger should be also considered in the cold start sequence. Post the boost assist there will be a pressure relief valve, which opens if both stages fail to control and regulate the pressure, this functions as a safety feature in the pressure

regulators. The outlet pressure setpoint was set to limit of 7 ± 1 barg. The high-pressure sensor measure tank pressure upstream the regulator. The pressure downstream can be measured in the rail sensor.

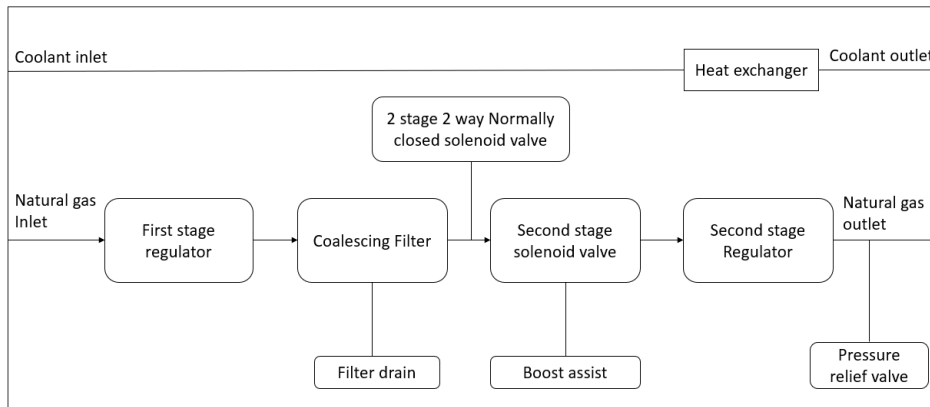


Fig. 1. 19 CNG pressure regulator functional block

1.7.5 LNG pressure regulator

The LNG pressure regulator is a single stage piston type regulator used in the Natural gas fuel metering system of spark ignition IC engines. The LNG regulator was designed to work in a system where the natural gas is stored in liquid phase (LNG, Liquified Natural gas) which then heated and supplied to regulator in the vapor phase. The main function of the LNG regulator is designed to prevent fuel rail pressure to maintain the pressure limits of the common rail to comply with the working conditions and working range of the gas injectors. The pressure regulator has to ensure the high flow rate at the LNG tank working pressure. The regulator was equipped with the **Shutoff valve (SOV)** at the inlet and the particulate filter (mesh) to filter in case of debris. The pressure regulator was connected with the (MAP) intake manifold of the engine in order to compensate the pressure, also the output order change based on the engine working conditions. This pressure regulator does not require the need of the Engine coolant circuit to warmup or to cool down. The pressure regulator works with the range of -40°C to 90°C . At ambient temperature the flow was measured at range of 20 kg/h

The permeability characteristics of the LNG pressure regulator depends on the input inlet pressure which will be compared to the nominal pressure.

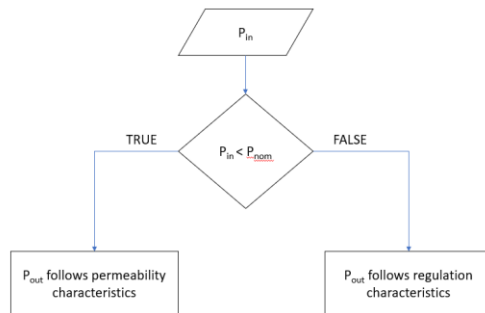


Fig. 1. 20 Operating characteristics of LNG regulator

Venting system/MAP reference: The hole is covered by the venting membrane to prevent dust, oil entering inside the chamber and the membrane is encapsulated to protection. Venting leaks from the dynamic lip seals to a specified area of the vehicle by a hose.

External Leakage: The total external leakage refers to leaks coming from all the points in the regulator system the rate is subject to limits of less than 15 Ncc/h according to regulation.

1.7.6 Pressure sensor and temperature sensor

The pressure sensor was attached to the common rail system, the pressure sensors are used as the reference measurement for the feedback loop for the controller, which helps to regulate the flow, but in case of the Natural gas application the pressure sensor is feed to the ECU but the output from the pressure regulator is constant. The temperature sensor measures the temperature of the gas, which was feed to ECU, which on CNG application required to control the heat exchanger to exchange the heat to maintain the optimum temperature in the circuit. Since the density and temperature have direct effect on the pressure.

1.7.7 Rail and Injectors

Rail (Multipoint Injection technology: direct mount on intake manifold): The common rail injector was used in the vehicle; the common rail injector incorporated the pressure and a temperature sensor, and the injectors are attached at the end of the the common rail. The injectors are placed on the intake port of the engine to prepare the stoichiometric mixture before entering the cylinder. The common rail was designed in such a way to reduce the pressure loss and equal pressure upstream the injectors, the end of the common rail contains a damping material to reduce the pressure fluctuation and avoid backpressure.

Material	Aluminium 6082
Internal volume	176 cm ³
Number of injectors	6
Injector type	Side feed injector, peak and hold
Optimum pressure	3 barg to 7 barg
Maximum allowed pressure	8 barg
Operating temperature	-40 °C to 100°C

Supply voltage to Pressure/temp sensor	5V
Maximum flow (Natural gas)	190 kg/h

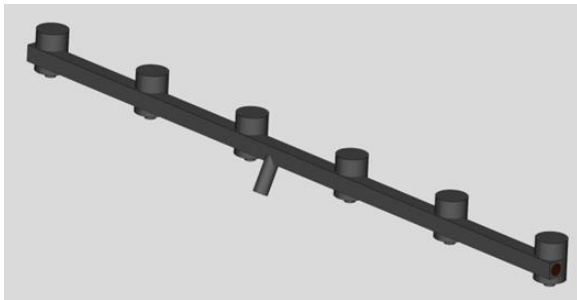


Fig. 1. 22 Common rail used in vehicle

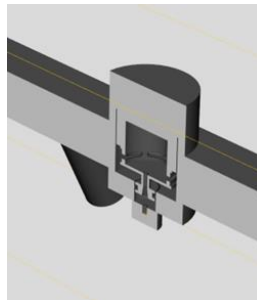


Fig. 1. 21 Cross section of side feed injector(B) assembly inside fuel common rail

The injectors work at the specified range of upstream pressure and temperature, which are necessary for the injector performance specified by suppliers, exceeding affects the injector nozzle, lift coefficient, armature, and coils which have impact on life cycle of the injector. The flow was determined by the engine fuel request and the injector capacity to allow the max flow capacity if the pressure regulator.

There are two injector model are used for the analysis: the first (injector A) used in the laboratory test bench to calibrate (12 x rail), validate the model and the second (injector B) used in the vehicle (6x rail). Both are solenoid injector with valve needle as moving assembly with armature and sealing element, the closing spring, and the valve seat.

Injector A: Top feed injector

The type A injector was used in the test bench for the calibration of the preliminary pressure loss model. The solenoid injector which contains the valve housing with electrical and the hydraulic connection, the coil (solenoid), the valve needle as moving subassembly with armature and sealing element, the closing spring, valve seat. The upper O ring seals against the leakage of the fuel from the common rail and the lower o ring prevents the leakage from cylinder to rail. The operation of the injector is performed via an Input and output injector driver. the nozzle size range between 3.0 to 3.2 mm in diameter. The opening time of 3.5ms and closing time 1 ms. It is possible to use the injector for peak and hold. The mass flow Q (kg/h) measure is only calculated value.

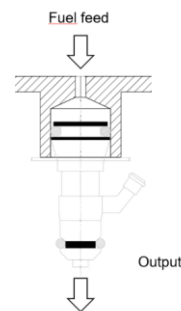


Fig. 1. 23 Injector A (top feed)

Injector B: Side feed injector (peak and hold)

The injector family fall under the category of side feed technology, where the single injector is feed with gas from the side pf the injector body while the outlet us realized in the bottom part of the injector. The gas pressure should be stabilized with in working range of 3.5 barg to 7 barg. The internal volume of the injector was divided into two segments which contains a mobile core inside. The volume upstream the sealing directly connected to the pressure regulator by the rail

and rubber hose and the volume downstream, the sealing is directly connected to the engine manifold by rubber hose. the nozzle size range between 3.0 to 3.2 mm in diameter. The opening time of 1.2 ms and closing time 1 ms , the where the minimum injection time will be 1.2-2.0 ms

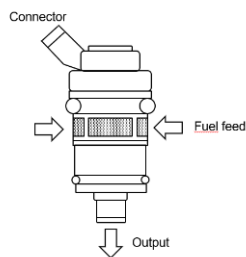


Fig. 1. 25 Injector B (side feed)

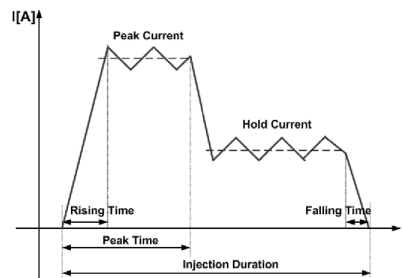


Fig. 1. 24 Peak and hold signal (injector B)

1.8 Problem statement

The scope of the thesis was to design and model 1D flow simulation using GT-SUITE tool to build a virtual model of the vehicle fuel line to measure the pressure loss at every local point in the system at engines different operating load conditions, which includes the temperature, pressure, and gas quality dependencies. The identification of the pressure loss in the circuit and the contributors are required to be measured, which then correlated with the data from the engine test bench and the vehicle.

To achieve the target, specific steps have been defined starting from simplified model representative of laboratory test bench till the vehicle model. Calculation has been validated with real data available.

Roadmap of Natural Gas circuit Design

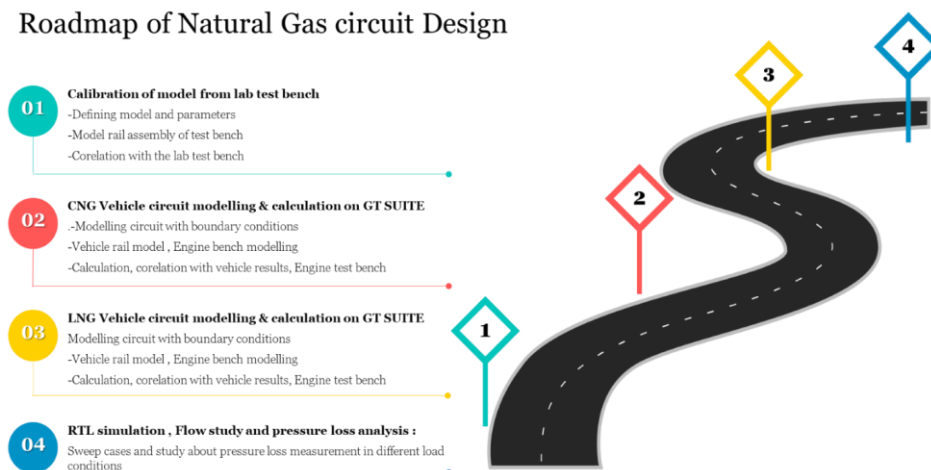


Fig. 1. 26 Roadmap journey of pressure measurement process for validation of the predictive pressure loss model

2 Laboratory test bench

1.1. Description

As first step, the goal was to design model with GT-Suite of the FPT Laboratory test bench minimizing the error based on the defined parameters.

The laboratory test bench was developed by FPT to run 1st level analysis on components. The test bench can be used either for development parts and returned parts from field (claimed parts) to check basic mechanical and electrical functionality of the injectors.

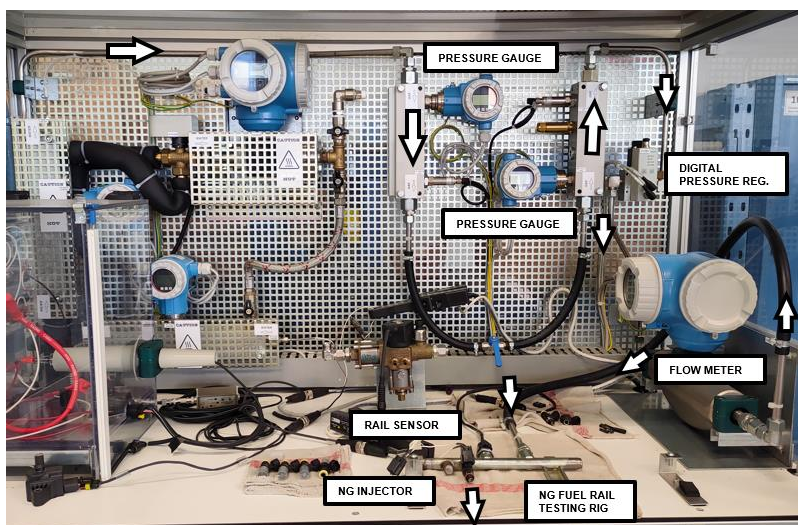


Fig. 1. 27 Laboratory test bench experimental setup (arrow indicate the flow path)

The bench layout is according to the figure below. The bench results read the pressure data in BarG and mass flow in Kg/h.

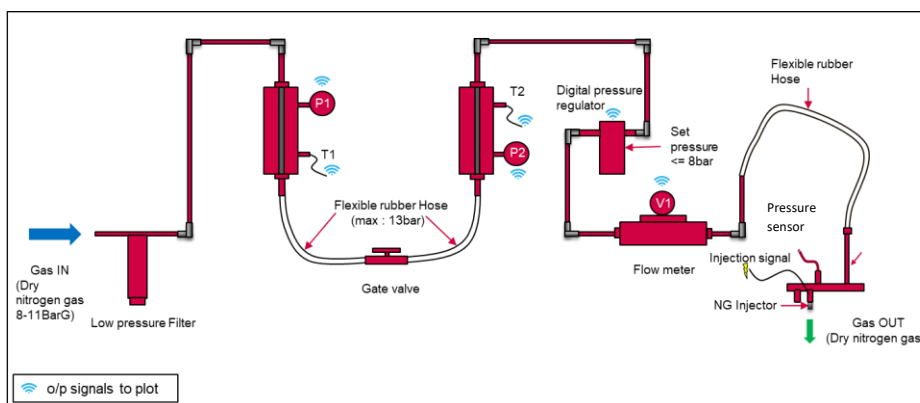


Fig. 1. 28 Schematic test bench layout featuring the components.

The bench is limited to operate with industrial Nitrogen gas at maximum 11 barG inlet pressure. Low pressure filter is present to avoid unintended contamination. Bench is currently not equipped with a pressure regulator but is foreseen to be placed instead of Gate valve present between (1) and (2). The digital pressure regulator is used to regulate the required pressure at rail. The digital pressure regulator works with the PID, PID controller is an instrument used in industrial control applications to regulate temperature, flow, pressure, speed, and other process variables. PID (proportional integral derivative) controllers use a control loop feedback mechanism to control process variables and are the most accurate and stable controller. The flow of Nitrogen is measured with a flow meter which captures the real time data in the system.

A simplified rail was used in the test bench to install different injectors and to compare the results for further analysis. The injector used in the test bench was natural gas injector A.

The simulation model was built in the GT-SUITE based on bench to calculate the pressure loss in the system under following boundary conditions:

Gas	Dry nitrogen
Inlet pressure	8 barg to 11 barg
Flow (adjusted)	Min 8 kg/h to max 12 kg/h
Set pressure in digital regulator	7 barg
Total length of pipe	3 m
Inner Diameter of pipe	8.5mm
Injector	Injector A
Test cycle for reference	100 Duty cycle (fully open)

Table 1. 5 boundary conditions

Model has been calibrated based on actual results from test bench and thanks to that it helps to predict results at higher pressure and flow conditions.

During the project approach, it has been faced the need to split the simulation in two steps indicated as follow:

- 1) High Level Simulation (*simplified circuit without orifice and complex connections*)
- 2) Deep Level Simulation (*considering all components in the circuit*)

Input gas pressure was read in the P1 and T1 in the circuit and the mass flow in case to mitigate the low-pressure conditions are used to implement using the valve which was connected with the circuit using a rubber hose. Then the downstream pressure can be, measured at the P2 and temperature at T2, the digital regulator set pressure was defined by the pressure which we should maintain in the common rail in our case the set pressure was defined as 5barG which was set as per the injector working range and the type of approval of the test to be conducted.

1.2. High Level Simulation

2.2.1 High Level Simulation: Description

The high-level simulation means we refer to a low-level model with simplified components. The GT SUITE 1D model was developed for the flow simulation. The flow model involves the solution of Navier-Stokes equations, specifically the conservation of continuity, momentum, and energy equations. These equations are solved in one dimension, which defines that all the quantities are average across the flow direction. There are two solutions we can get the results depends on the

method to capture high frequency waves such as in injection systems on time integration methods:

- 1) Explicit solver
- 2) Implicit solver

The explicit method requires small time steps, this solver is opted for simulations where the unsteady flow, high frequency, pressure pulsations, wave dynamics are the area of interest. The Simulation takes time step in order of 0.001s to 0.01s. It takes huge computational cost and time for the solver in order to capture high pressure signals, which is the area of interest for the pressure loss study in the rail and injectors.

Implicit solver variable such as mass flow rate, pressure and total enthalpy are calculated by solving nonlinear system to find values of the sub volumes at current time step simultaneously. The time step can be in order of seconds to minutes, this simulation is useful for longer simulations. This reduces the Computing cost.

The following equations are governing pressure drop measurement units.

- 1) Darcy formula: used for non-compressible flow such as oil, water, and other liquids in pipe. In case of compressible fluid (e.g., natural gas that we are considering), when the pressure drop is less than 10% of P_1 (inlet), use ρ based on either inlet or outlet conditions. When the pressure drop is greater than 10% of P_1 (inlet) to 40% of P_1 (outlet), we should use the average of ρ based on the inlet and outlet conditions.
- 2) Weymouth formula: used for fluid in small pipes and high-pressure gas.

$$q'_h = 0.00261 d^{2.6182} \sqrt{\frac{(p'_1)^2 - (p'_1)^2}{S_g L_m} \left(\frac{288}{T}\right)}$$

1D model and scheme are summary reported below.

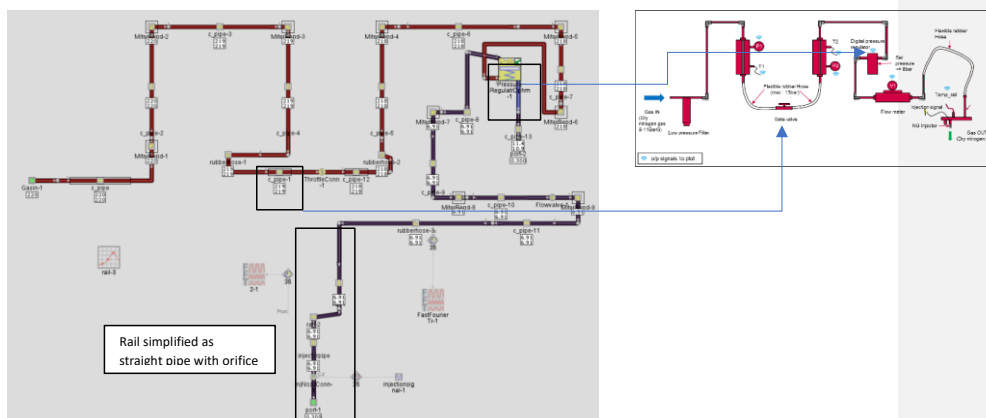


Fig 2. 1 Layout of the test bench designed and imported in the GT SUITE model

The model is done in simplified version eliminating complex connections, small converging, and diverging profiles. The digital pressure regulator is modeled as the diaphragm pressure controller. See below table for summary boundary conditions.

The angle of gate valve is corrected to obtain pressure buildup in the rail with desired the gas flow in the circuit. The simplified circuit represents the single injector of the vehicle, which imposes the duty cycle of injector with respect to the different engine RPM. For the initial study the 100% duty cycle was considered since the exact injection timing of the engine for RPM of the engine was not known at this stage. Thus, with available data and, at engine level, it can be correlate to engine speed. 60° of gate valve open corresponds to flow of Nitrogen in the circuit which can meet the injector A maximum constant flowrate.

2.2.2 High Level Simulation: Boundary conditions

The simulation was setup in order to inject the maximum flow allowed by the injector at 100% duty cycle in one cycle. Thus, different engine speed cases have been investigated to simulate different flow conditions. See below table as reference for overall boundary conditions.

Main						
Parameter	Unit	Description	Case 1	Case 2	Case 3	Case 4
Case On/Off		Check Box to Turn Case On	<input checked="" type="checkbox"/>	<input checked="" type="checkbox"/>	<input checked="" type="checkbox"/>	<input checked="" type="checkbox"/>
Case Label		Unique Text for Plot Legends				
pipeinletdia	mm	Diameter at Inlet End	8.5...	8.5...	8.5...	8.5...
waltemp	C	Imposed Wall Temperature	20...	20...	20...	20...
railinlet	mm	Diameter at Inlet End	12...	12...	12...	12...
pgasin	bar	Pressure (Absolute)	11...	11...	11...	11...
poutambient	bar	Pressure (Absolute)	0.3...	0.3...	0.3...	0.3...
rpm	RPM	Rotational Speed	6000...	5000...	2000...	1000...
angleofopen		Throttle Angle (30/45/60/90)	60...	60...	60...	60...

Fig 2. 2 test case and boundary condition of laboratory test bench

2.2.3 High Level Simulation: Results

First degree approximation model run to check the basic working principle of the circuit. The model ran without errors, due to high pressure oscillations the implicit solver cannot be used, explicit solver was used with driver 720 degree considered in the GT SUITE run setting. Under boundary conditions, the first results are plot on next chart. The choice to measure the pressure loss in the mass control pipe to understand the pressure changes and control happens in the pressure control valve at different flow conditions with respect to engine rpm (high flow to low flow)

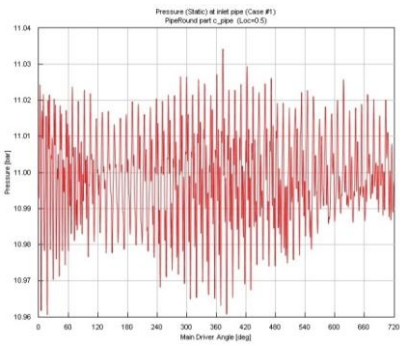


Fig 2.3 case1: pressure measured at control valve

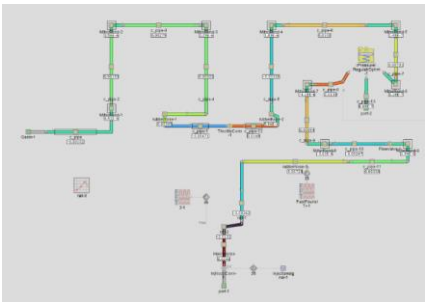


Fig 1.4 case 1: circuit pressure

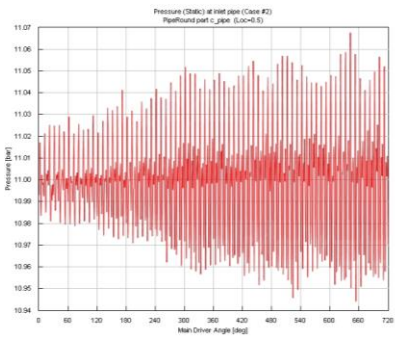


Fig 2.5 case2: pressure measured at control valve.

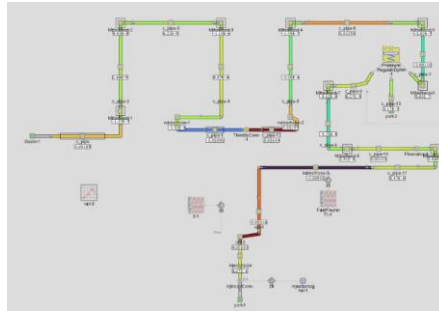


Fig.2.6 case2:circuit pressure

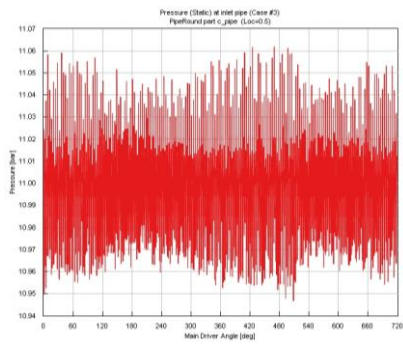


Fig 2.7 case3: pressure measured at control valve.

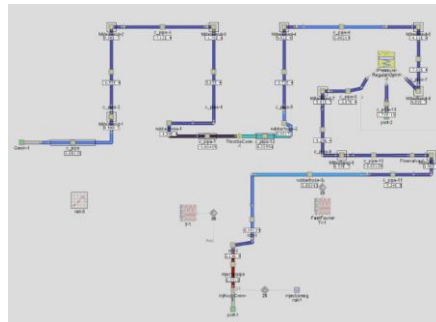


Figure 2.8 case3:circuit pressure

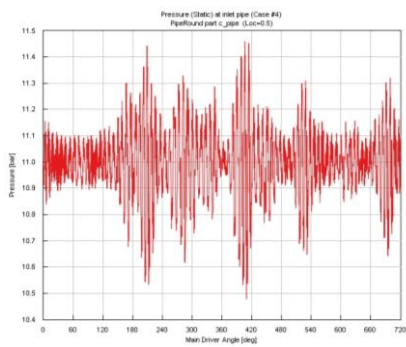


Fig 2.9 case4: pressure measured at control valve

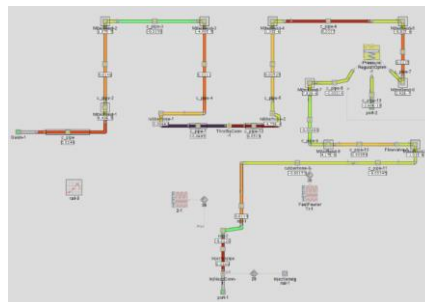


Figure 2.10 case4: circuit pressure

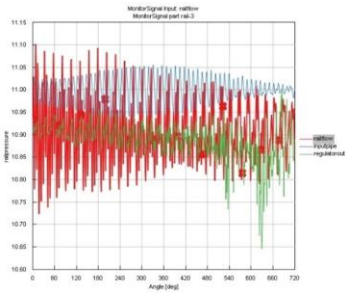


Fig 2.11 monitored signals of mass flow in rail, pressure input, regulator output.

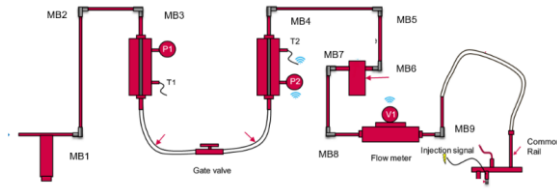
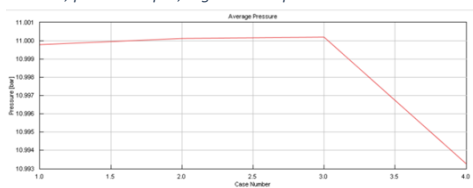
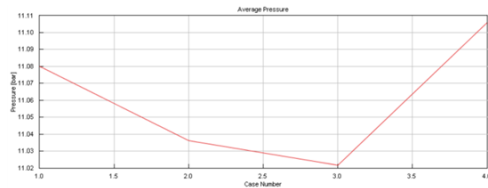


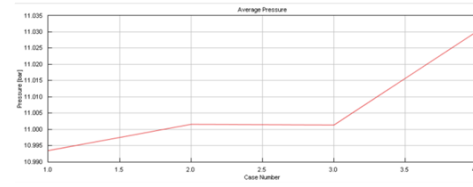
Fig .2.12 test bench layout showing MB(mitre bends)



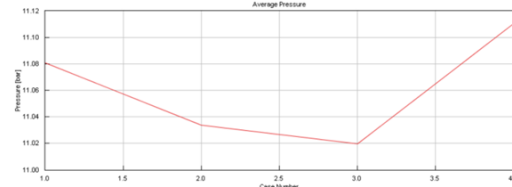
Pressure(static) Mitter bend 1 [ALL CASES]



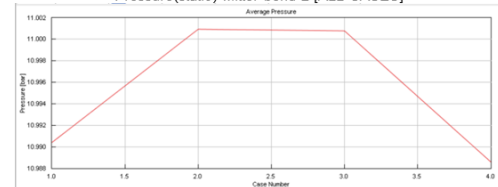
Pressure(static) Mitter bend 4 [ALL CASES]



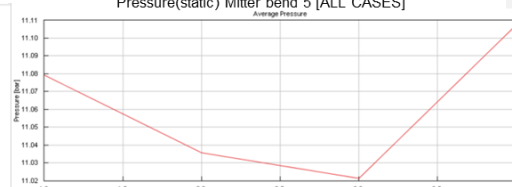
Pressure(static) Mitter bend 2 [ALL CASES]



Pressure(static) Mitter bend 5 [ALL CASES]



Pressure(static) Mitter bend 3 [ALL CASES]



Pressure(static) Mitter bend 6 [ALL CASES]

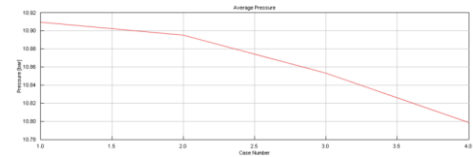
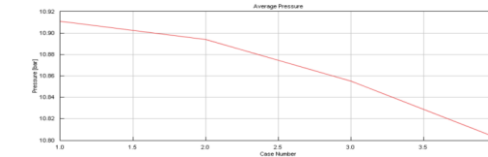
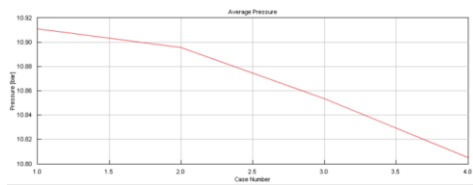


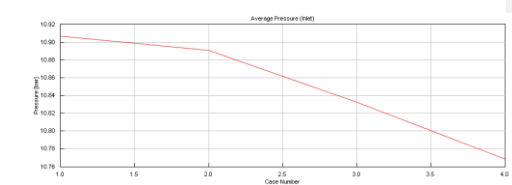
Fig. Pressure(static) Mitter bend 7 [ALL CASES]



Pressure(static) Mitter bend 9 [ALL CASES]



Pressure(static) Mitter bend 8 [ALL CASES]



Pressure(static) RAIL [ALL CASES]

From the initial test, the individual contribution of the pressure loss factor was tried to understand and model validity was identified with the test bench. The constant pressure *inlet 11 barg* was given to the circuit and the mass flow was kept at constant range *11.4 kg/h* to identify the pressure variation due to connections, sharp bends, length of pipe, varied sections in the circuit. The injector was modelled as a simple opening considering the cross section of the injector which the data was supplied. Since we have external measurements, it was easy to predict the chamber volume inside the gas injector which was evaluated and added to the model. Here for the uniform flow the 100 Duty cycle of the injector was considered to validate the flow. Which the above data the first approximated model was design, and the results are plotted with the contribution of pressure loss at every pipe in the circuit.

Different flow conditions corresponding to different engine speed has been simulated and results plot below.

Components and Connections	Case #1 11.4 Kg/h at 6000 rpm Pressure loss [bar]	Case #2 11.4 Kg/h at 5000 rpm Pressure loss [bar]	Case #3 11.4 Kg/h at 2000 rpm Pressure loss [bar]	Case #4 11.4 Kg/h at 1000 rpm Pressure loss [bar]
C_pipe	0.02	0.02	0.04	0.07
Miterbend-1	0.14	0.14	0.29	0.42
C_pipe 2	0.15	0.15	0.30	0.46
Miterbend-2	0.14	0.14	0.28	0.42
C_pipe-3	0.15	0.16	0.31	0.46
Miterbend-3	0.14	0.15	0.28	0.43
C_pipe-4	0.15	0.15	0.30	0.46
Rubberhose-1	0.12	0.12	0.23	0.36
C_pipe-1	0.006	0.006	0.01	0.02
throttleConn-1(angle60)	0.49	0.51	1.01	1.52
C_pipe-12	0.007	0.007	0.014	0.02
Rubberhose-2	0.1	0.11	0.23	0.34
C_pipe-5	0.1	0.15	0.29	0.45
Miterbend-4	0.14	0.14	0.28	0.42
C_pipe-6	0.03	0.04	0.07	0.11
Miterbend-5	0.14	0.14	0.28	0.42
C_pipe-7	0.06	0.06	0.114	0.17
Miterbend-6	0.14	0.14	0.28	0.43
Injector pipe	0.001	0.001	0.001	0.002
Cumulative P_{drop}	2.26	2.34	4.62	6.96

Table 2. 1 Individual pressure loss contributors in the test bench circuit

Considering above results the highest-pressure loss have been identified on following points of the circuit:

1) Throttle connection

2) Mitter bend 1 to 6

3) the rubber hose losses changes with respect to the position it kept for testing, loss depends on the radius maintained.

Out of the first approximation model results, the case 3 and case 4 are completely out of range since the model overestimates the pressure loss and error shoots up. Thus, fine tuning of model and simulation parameters have been carry-out into the Deep Level Simulation. From the circuit we obtained close pressure output from the rail, so this model was almost predicting the pressure behavior with limited data. So, the next step will be building the exact design of the circuit to obtain the exact pressure output on the rail and mass flow at steady input pressure.

1.3. Deep Level Simulation

2.3.1 Deep Level Simulation: Description and Boundary conditions

Keeping the boundary conditions same as high level simulation, more precise model has been done here to replicate the exact physical dimensions of common rail, injector, pipe, pressure regulator, connectors, and material properties. Detailed modeling allows also to replicate the real relevant dimensions such as orifice, sharp bends, and convergences. See below table as reference.

Part	Material	Dimensions previously used in highlevel	Corrected Dimensions (Deep level)
Metal pipe	Stainless steel	8.5 mmx1.6 mm	$\varnothing 8.85 \pm 0.1 \times 1.5$ mm
Rubber Hose	Nitril Rubber (Acrylonitrile-butadiene rubber)	8.5 mm	$\varnothing 8.80 \pm 0.1 \times 2.5$ mm
Connectors	Stainless steel	8.5 mm	$\varnothing_{ID} 12 \pm 0.1$ mm
90° Bend	Stainless steel	10 mm x 40 mm x 40 mm	$\varnothing_{ID} 12 \pm 0.1 \times 36.65$ (L) x 35(L) mm
Rail	Volume (stainless steel)	Straight pipe (8.5x26.5mm)	63364.49 mm^3 / 63.36ccm

Table 2. 2 Dimensions and material properties

The physical parts have been measured and CAD model has been replicated as shown in drawing below



Figure 2.15 common rail detailed drawing



Injector was modelled as an orifice nozzle with the calculated cross section of the hole of the injector and resulting simulation model into GT SUITE is reported on next picture.

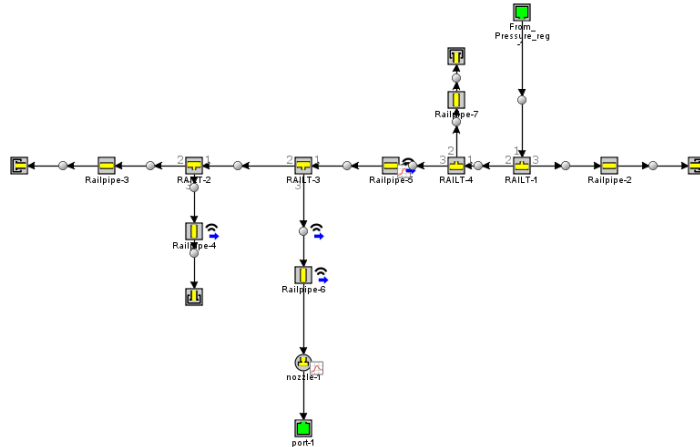


Fig 2. 16 1D rail model used for simulation

We have known Nozzle diameter, but discharge coefficient and the friction factor have to be identified which was evaluated with DOE (design of experiments) approach to match the mass flow of nozzle characteristics to minimize the error versus laboratory results. See following picture for GT SUITE model used.

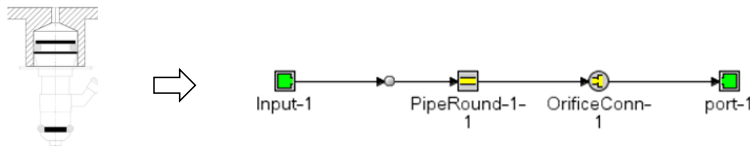


Fig 2.17 Nozzle and injector simplified as pipe and orifice in GT SUITE to calibrate with optimisation

To calibrate the model an automatic calculation routine has been implemented (integrated optimizer design).

2.3.2 Deep Level Simulation: calibration of the model out of integrated design optimizer

I have calibrated the calculated model focusing on injector and rail to minimize the error percentage of the mass flow at different pressure level in the common rail. The inbuilt function of design optimizer was used to set the model to reach the target mass flow rate by different case sweep.

Thus, with running 10 cases with different data from the bench the model was used to optimized to match the best fit discharge coefficient of the nozzle. After running 194 iteration of the 10 cases, similarly, run was simulated for 3 types of output from the bench. In total 194*3 test cases are run in the GT-Optimizer to obtain the optimized forward and reverse discharge coefficient.

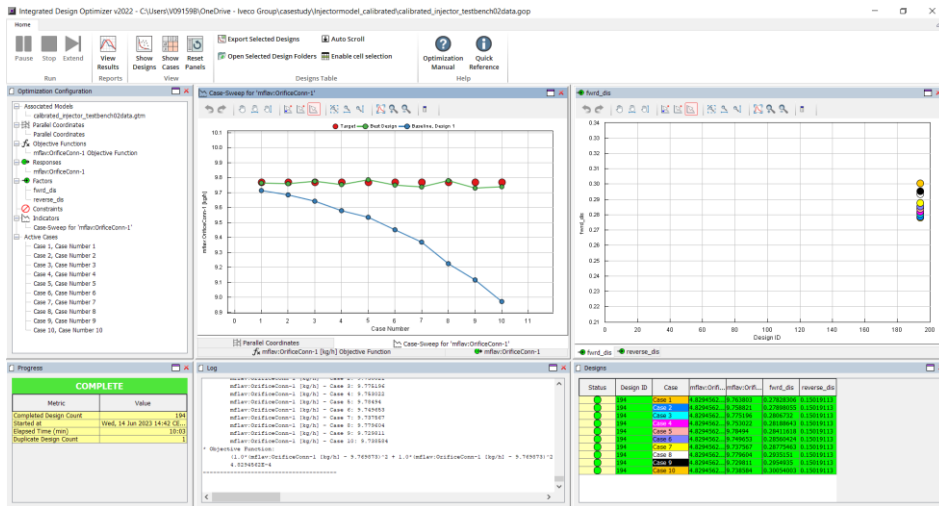


Fig 2.18 Integrated Design Optimizer in GT SUITE used to calibrate the injector nozzle

2.3.3 Deep Level Simulation: Injector nozzle model validation

Results of simplified model of the Injector Nozzle validation to minimize the error are reported below.

Iteration 1: forward coefficient: 0.2758 & reverse coefficient 0.2304

Pressure rail (barg)	Mass flow (experimental) (Kg/h)	Mass flow simulated (Kg/h)	%Error
7.49	9.67	9.67	0.05
7.47	9.75	9.65	1.10
7.44	9.86	9.60	2.70
7.40	9.87	9.54	3.42
7.36	9.94	9.50	4.68
7.30	9.95	9.41	5.74
7.24	9.81	9.33	5.17
7.14	9.70	9.19	5.55
7.06	9.66	9.08	6.40
6.95	9.43	8.94	5.53
		Average error Percentage	3.98

Table 2. 3 compared results between measured and simulated mass flow with reference to pressure in rail

Iteration 2: Forward discharge coefficient: **0.2768** and reverse discharge coefficient **0.1409**

Pressure rail (barg)	Mass flow (experimental) (Kg/h)	Mass flow simulated (Kg/h)	%Error
7.495	9.674	9.713	0.40
7.477	9.756	9.684	0.75
7.445	9.867	9.642	2.34
7.400	9.872	9.578	3.06
7.369	9.946	9.534	4.32
7.307	9.958	9.450	5.37
7.247	9.818	9.368	4.80
7.142	9.703	9.224	5.19
7.065	9.666	9.116	6.03
6.958	9.435	8.971	5.17
		Average error Percentage	3.62

Table 2. 4 compared results between measured and simulated mass flow with reference to pressure in rail

Finalized values: Forward discharge coefficient **0.2789** and reverse discharge coefficient **0.1502**

Pressure rail (barg)	Mass flow (experimental) (Kg/h)	Mass flow simulated (Kg/h)	%Error
7.495	9.674	9.763	0.92
7.477	9.756	9.758	0.02
7.445	9.867	9.775	0.95
7.400	9.872	9.753	1.22
7.369	9.946	9.784	1.65
7.307	9.958	9.749	2.14
7.247	9.818	9.737	0.83
7.142	9.703	9.779	0.78
7.065	9.666	9.729	0.66
6.958	9.435	9.738	3.12
		Average error Percentage	0.13

Table 2. 5 compared results between measured and simulated mass flow with reference to pressure in rail

So now we have the optimized model of the injector and the nozzle which represents the complete injector model. Now we have to optimize the the injector assembled with the common rail, so we get the complete model of common rail with the injector as whole.

2.3.4 Deep Level Simulation: Rail assembly model validation

Now, model should be developed with common rail and optimized injector in the lab test bench model. The exact pipe dimensions, connectors and the bends are measured and modelled, then the model was linked with the optimized nozzle of the NG injectors. Once the model was validated this model was opted to predict the flow rates at different input pressure. The following figures are obtained during optimization during GT SUITE.

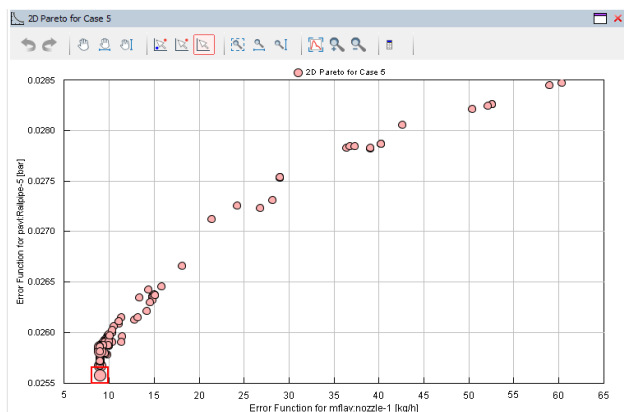


Fig 2.19 Trading off error function of nozzle mass flow vs Error function of pressure in rail

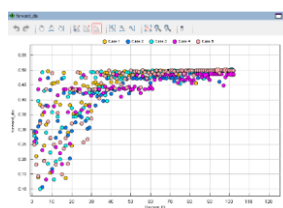


Fig 2.20 forward discharge coefficient

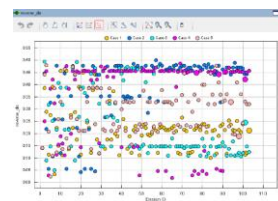


Figure 2.21 Reverse discharge coefficient

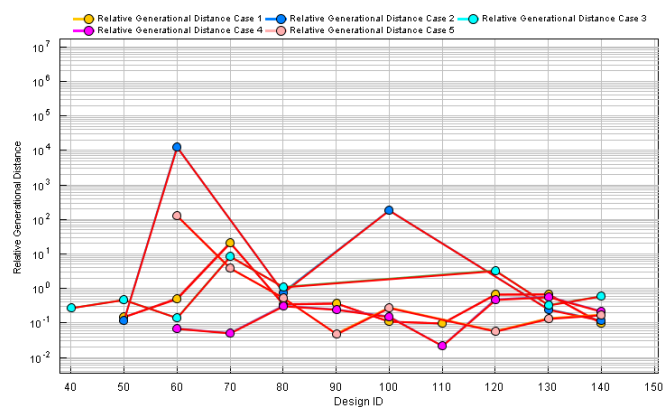


Fig.2.22 convergence of case1, case 2, case 3, case 4, case 5

Here we can notice the error function of rail pipe against the error function of mass flow in the nozzle these two parameters should be as low as possible to obtain the lowest error in the prediction model, for this we tune again the forward and reverse discharge coefficient with complex circuit.

The pareto chart shows the trade off in selection of Error function of flow rate vs error function of rail pressure. The results are plotted and the best discharge coefficients very close to the experimental data are selected and evaluated again with different input pressures in the test bench and analyzed results are plotted. Thus, it is possible to evaluate the model with prediction capability and the error functions or offsets with was evaluated, which the offset function can be added to the results to get the accurate results.

The below table is the result of the error in the mass flow of the circuit measured in the circuit with the simulation results from the GT-Suite and the experimental measurements taken from the laboratory test bench, thus we compare the error percentage in total. Each data of the experimental data was the result of average of three test run on the lab. Thus, these average changes from injector to injector based on the error tolerance of the injector model itself.

INPUT PRESSURE (dry Nitrogen)	Mass flow measured in the rail		% Error	Pressure amplitude in rail		% Error
	Experimental Flow (kg/h)	simulation Flow (kg/h)		Experimental (barg)	simulation (barg)	
P_input (Barg)						
7.578	9.731	9.754	0.23	7.461	7.557	1.28
7.577	9.736	9.753	0.18	7.464	7.556	1.24
7.594	9.719	9.775	0.57	7.467	7.573	1.41
7.025	9.286	9.043	2.62	7.038	7.006	0.45
7.1456	9.439	9.199	2.54	7.141	7.126	0.21
7.072	9.290	9.104	2.00	7.076	7.0529	0.32
6.974	9.220	8.978	2.63	6.997	6.955	0.60

Table 2. 6 Error percentage evaluation of the laboratory test bench vs simulation of tuned common rail with injector

The output we obtain from the model is already closer to the experimental data. The model was pushed outside the working range to evaluate its capability for handling the error. Outside the working range it is able to predict the error at the offset rate of **3.0% to 16%**. whereas within range of rail pressure the range of error was **0 % to 1.5%**. Thus, this model has the capability to predict the different components, thus the local pressure loss contributions are recorded. This gives more agility to test different components if we evaluate or know the discharge coefficient, we don't need to set up test bench every time, since the model have more capability to measure all the data's such as performance of the flow, back pressure, pressure loss, density variation. The model can also be introduced with different input gas, since the test bench results are converted from nitrogen to methane manually post experiment, but with the model we have it gives us the edge to evaluate with methane gas with different quality, compositions, which can be also measure the different duty cycle of injector. If it is possible to get the data of armature, moving rod mass, spring stiffness of the injector, it is easy to build the injector model and evaluate the hysteresis curve to evaluate accurate flow per injection cycle at different duty cycle with more accuracy, this gives exact feedback on the engine performance without dependency of the exhaust, turbo components. Which makes to tune the injection offset time to achieve more complete combustion cycle.

2.3.5 Deep Level Simulation: Model validation and Results

The laboratory test bench was used to measure the different types of tests which was imposed on the injectors to measure their different operating conditions, these test cycle contains certain test such as high voltage, peak and hold, duty cycle, these are performed to observe and test the products (injectors). But for the development of the model the 100 duty cycle data was used taken tune the model, the window of operation in range 30s to 40s of the test. The below image represents the complete test cycle coming from lab bench.

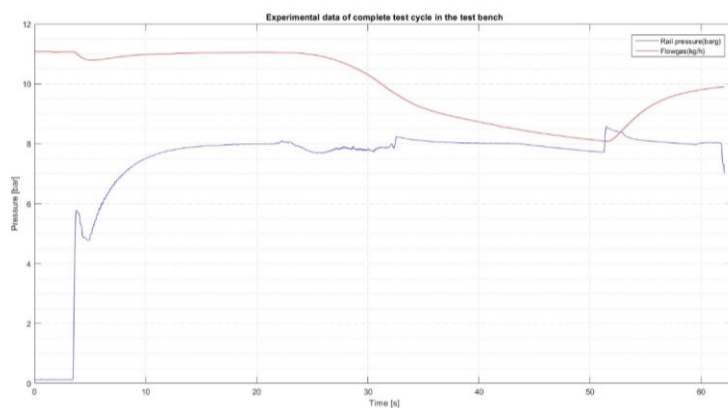


Fig 2.23 Experimental data of the complete test cycle in the test bench

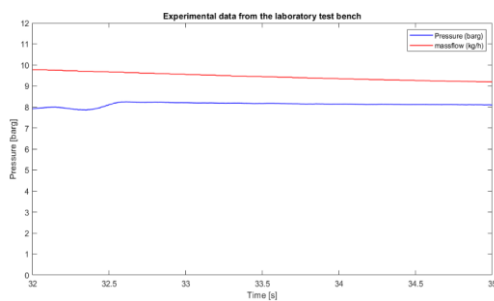


Fig 2.24 Results from the GT Suite simulation (Inlet pressure barg vs flow gas (kg/h)) for given input pressure measured in rail of the- laboratory test bench model.

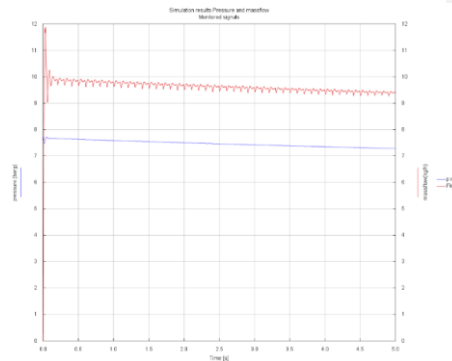


Fig 2.25. Simulation results from GT Suite for t=5s at 100 Duty cycle (32s to 35s in test bench data match with simulation)

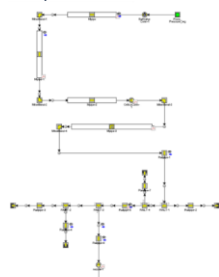


Figure 2.26 GT SUITE complete layout of the laboratory test bench for reference

Validation of model was done testing the working range of the test bench:

- The optimal condition for the rail pressure tuned for working range was 7 barG \pm 0.7 barG with working fluid (Dry Nitrogen) at 23°C
- The model was pushed outside the working limit of the rail pressure [6.8 to 9.6 barG]

Input pressure (barG)	Experimental Flow (Kg/h)	Simulation Flow (Kg/h)	% Error
8.13	9.85	10.44	5.98
7.97	10.09	10.26	1.71
7.57 (upper limit)	9.73	9.75	0.24
7.57	9.74	9.75	0.19
7.59	9.72	9.78	0.58
7.02	9.29	9.14	0.53
6.98	6.88	6.79	1.30
6.82 (lower limit)	9.11	8.98	1.33

Table 2. 7 Percentage of error from experiment and simulation

The model was tuned with the injector of maximum flow which was specified by injector A considering the tolerance limit of variation, this model is working in optimum condition trying to converge the results. The model outside the boundary conditions can be verified in the test bench with the different setting pressure in the digital regulator so that the results outside the boundary conditions can be verified.

Conclusion from lab test bench result:

- The Test bench circuit was completely modelled and validated using the experimental analysis and the data from the laboratory test bench
- The Limitation of the model was inside the working range of the tuned Injector model as per the supplier specifications where the part itself incorporated error tolerance
- The model optimized to work in the range of P_{rail} **6.8 to 9.6** barg of varied input pressure

WORKING PRESSURE RANGE (barg)	ERROR (Percentage)
6.40 – 6.80 (Lower limit)	0.0 % to 4.0%
6.80 – 7.50 (Working range)	0.0 % to 1.5%
7.51 – 7.90 (Upper Limit)	0.0 % to 3.0%
7.91 – 9.2 (out of limit)	3.0 % to 16 %

Table 2. 8 Simulation model of combined average of P_{rail} and Error percentage by correlating with the test bench results

For the further improvement can be achieved with the injector with the needle lift profile, it is possible to evaluate the delay in the opening profile and the injection (kg/h) can be evaluated. Which gives the correct mixture ratio of fuel as per the engine load requirements. Since the objective of thesis was to evaluate the pressure loss in circuit, the injector model was simplified to check the flow conditions in the length of the circuit.

1.4. Layout optimization investigation

In effort to reduce the pressure loss in the circuit, it is necessary to study the feasibility of change of pipe diameter, then the study was completed by running with close diameters by increasing in steps to identify the pipe diameter with maximum fuel flow with minimum pressure loss. Post selection of diameter the study was conducted by changing the material of the connecting tube to the rail from Rubber hose to flexible metallic pipe section.

2.4.1 Pipe diameters sweep study (explicit solver)

In order to evaluate the difference in pressure loss involved in the pipe diameter as a variable the study was conducted with the validated model. The next phase of the process was to redesign the test bench circuit to reduce the loss upstream the rail. Thus, to stabilize the pressure through the entire circuit and reduce the fluctuation and back pressure in the circuit. The pipe dimensions used varied from 7 mm ,8 mm, 8.5 mm, 9 mm, 9.5 mm, 10 mm. all the plots are evaluated carefully to understand the if sonic chocking occur in the system.

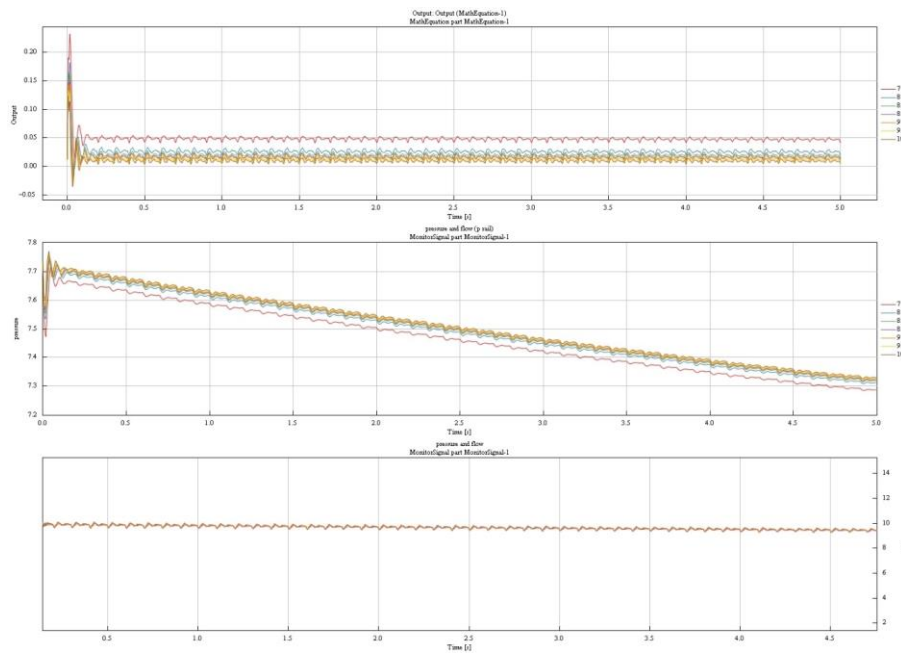


Figure 2.27 i) pressure drop due to backpressure near input pipe ii) Pressure drop measured in the rail iii) mass flow measured in the common rail

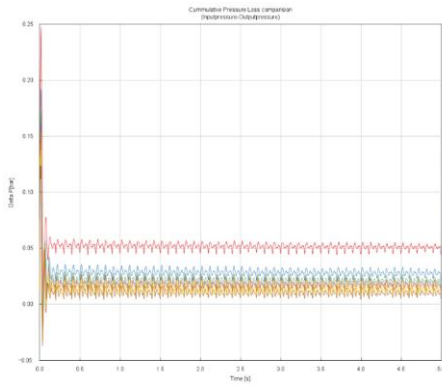


Figure 2.28 cumulative pressure loss between varied cross section study

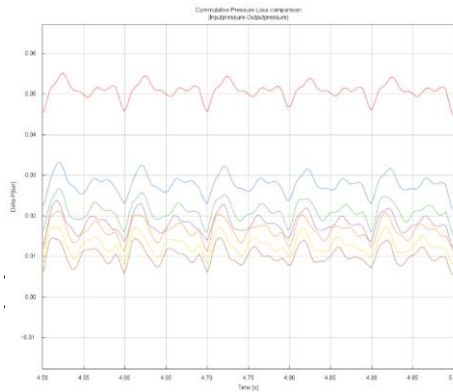


Figure 2.29 Cumulative pressure loss magnified section

Case study was conducted by taking the three cross-sections of the pipes (7mm, 8mm,9mm) with constant pressure input of 7 barg and the pressure loss is measured

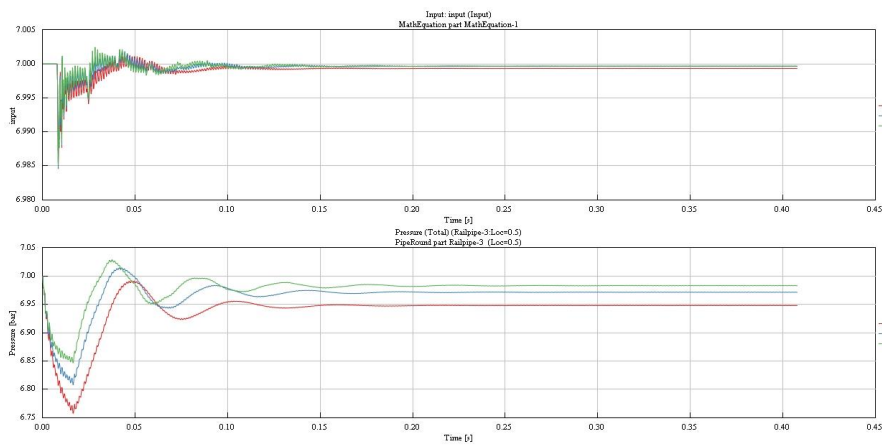


Figure 2.30 (top)-Input boundary pressure of pipe diameter 7mm,8mm,9mm (Bottom)- common rail pressure measured due to changes in upstream pipe diameter 7mm,8mm,9mm

The above graph indicated that the input pressure, which was given in the circuit remains close, but the pressure measured at the common rail pipe shows a wide difference, this show that requirement to avoid the small diameter pipe in the event of long circuit connections, however this pressure changes and recovers in the circuit depending on the design of the circuit.

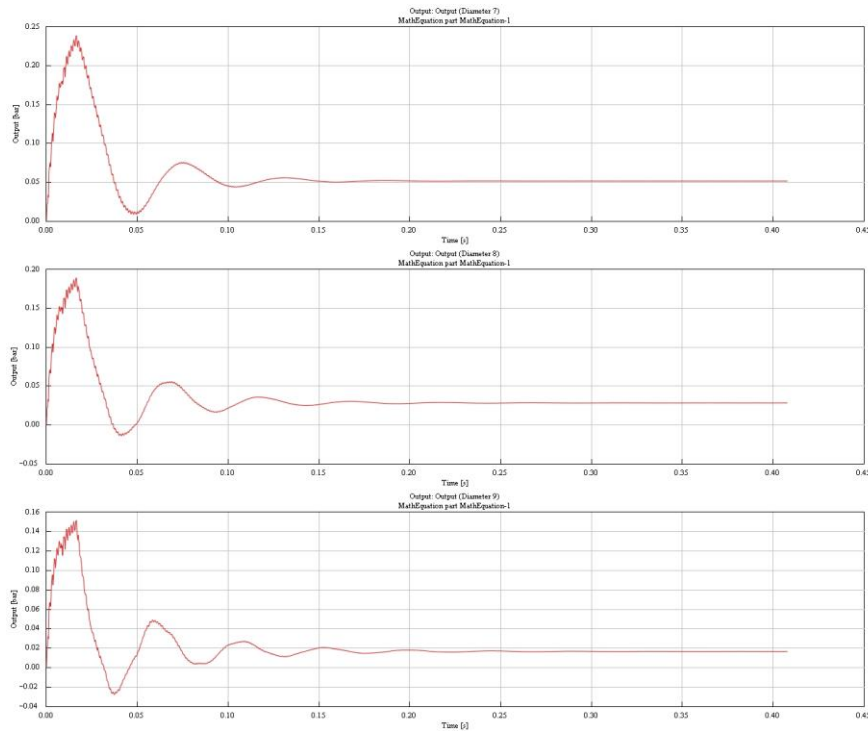


Figure 2.31 i) Total pressure loss measured in the rail input at diameter 7 mm ii) Total pressure loss measure in the rail input at diameter 8 mm iii) Total pressure loss measure in the rail input at diameter 9 mm

The above graph represents the total pressure loss which was measured along the input of the rail connection, here it is clear that we can note the loss is very easy to observe, the high diameter pipe (9 mm) which has the loss equivalent close to zero, this was measured at steady state condition, but when the injector opens and closes at high frequency the loss was measured at high amplitude

The below graphs are obtained as the result of pressure measurement from the fig 2.7.6 scheme as shown here. These pressure measurements are measured in the highlighted sections of the test bench circuit layout specifically at four miter bends where the loss is maximum compared to the other parts in the circuit.

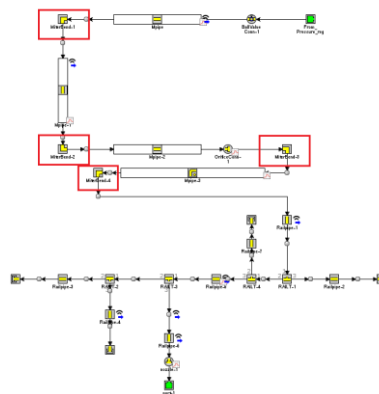


Figure 2.32 lab test bench layout for reference (highlighted Miter bends)

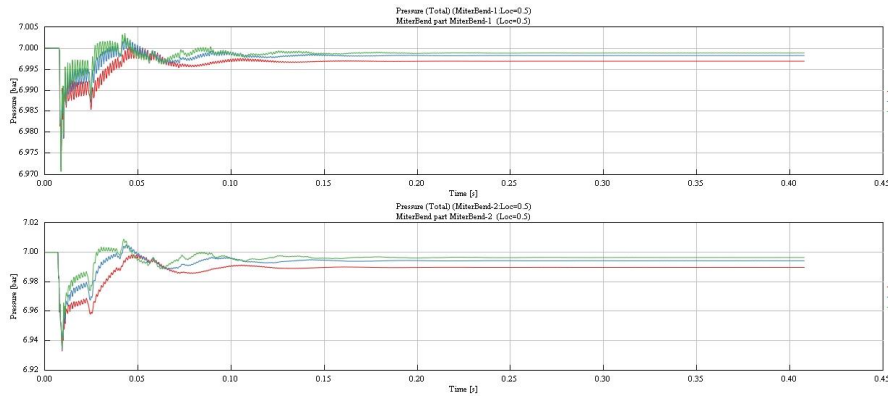


Figure 2.33 i)(above) Pressure measurement at miter bend-1 of 3 diameters 7mm,8mm and 9mm ii)(below) Pressure measurement at miter bend-2 of 3 diameters 7mm,8mm and 9mm

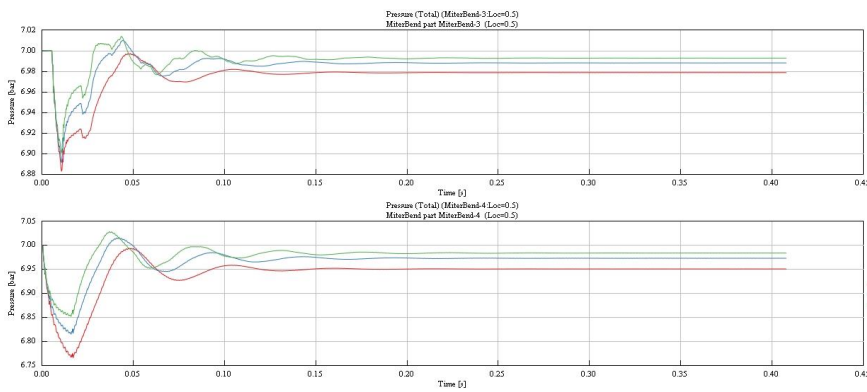


Figure 2.34 i)(above) Pressure measurement at miter bend-3 of 3 diameters 7mm,8mm and 9mm ii)(below) Pressure measurement at miter bend-4 of 3 diameters 7mm,8mm and 9mm

2.4.2 Pipe material study

After the results from the miter bends are obtained ,the comparison study was carried out to reduce the loss by removing the rubber hose , which acts as a damping system in the system, but in reality this damping effect does not exist in the vehicle thus to check the pressure fluctuations the test was carried by comparing results with rubber hose and by replacing rubber hose with metallic hose (stainless steel) cross section.

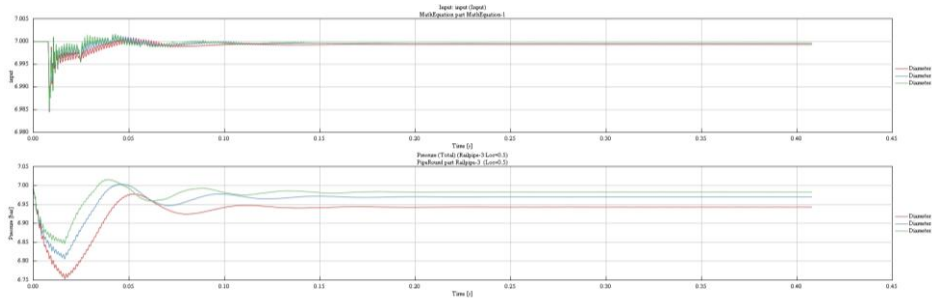


Figure 2.35 i) Input pressure at boundary measured at different diameter pipe 7mm,8mm,9mm ii) (below) pressure measured in common rail connecting tube (Nitrile rubber tube)

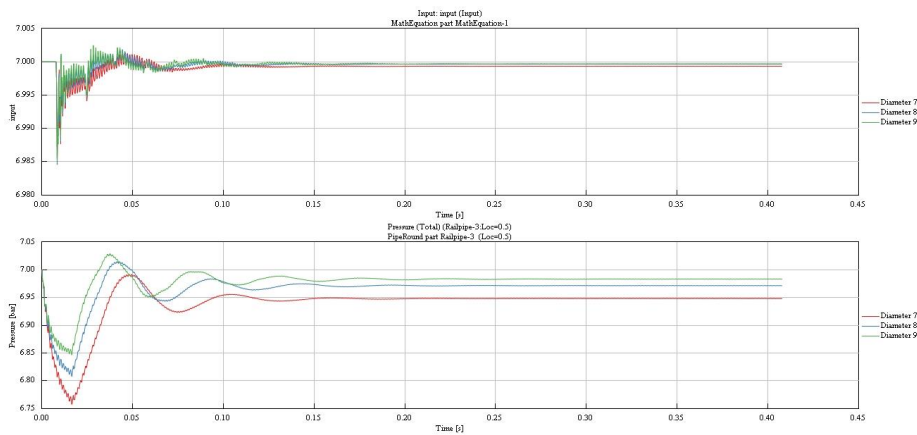


Figure 2.36 i) input pressure at boundary measured at different diameter pipe 7mm,8mm,9mm ii) (below) pressure measured in common rail connecting tube (stainless steel)

From the comparison between the two different materials the important outcome is

1. The usage of nitrile rubber hose was subject to expansion of diameter along the walls, such that the pressure variation differs depending on the young's modulus of the rubber material (elastomer compound)
2. The elastomer used in the rubber hose reduces the peak pressure waves and damped it which has a vital effect in the travelling waves this improves the high-speed operating condition and avoid the sonic choking phenomenon
3. The metallic tube on the other hand cannot damp the peak pressure waves but the pressure loss in tube is almost 0.5 bar per meter of the pipe, thus it multiplied when the length was increased with bend radius.
4. As we increase the diameter of the tube it is possible to obtain reduced pressure loss, thus opting the diameter 9 mm of the tube substantially reduced the cumulative pressure loss as per the observation.

2.4.3 Suggestion for test bench improvement

From the results there are very minor difference in the pressure loss and in the rubber hose, but the damping effect was comparatively indifferent compared to the engine layout since the material used in the vehicle was different. The suggestion was to keep rubber hose in the test bench to keep the ease of access to connect and disconnect the components from the system, but the length should be kept as reduced as possible to reduce the unintended bends or short radius. From the suggested configuration the miter bends are reduced from 9 no. s to 4 no.s, which reduced the loss almost 50%, implementing the short rubber hose reduce the loss contribution. This is also because the rubber hose has the possibility to change its internal cross-section which expands and contracts, even though the expansion was limited to 0.2mm in diameter, 0.2mm*1000mm in total volume difference occurs. Thus, this should also take into consideration. It is important to measure the young's modulus and elasticity of the rubber components to analyze the behavior.

We can notice the spike at the beginning of the simulation which is due to the velocity of the gas flow into system due to sudden opening of the injector, thus when injector was operated in the regular actuation $t = (0.02s - 0.05s)$ frequency the pressure waves propagate in the circuit ,thus keeping the circuit as close as possible and reducing the damping parts can converge the close results to identify and eliminate the choking effect

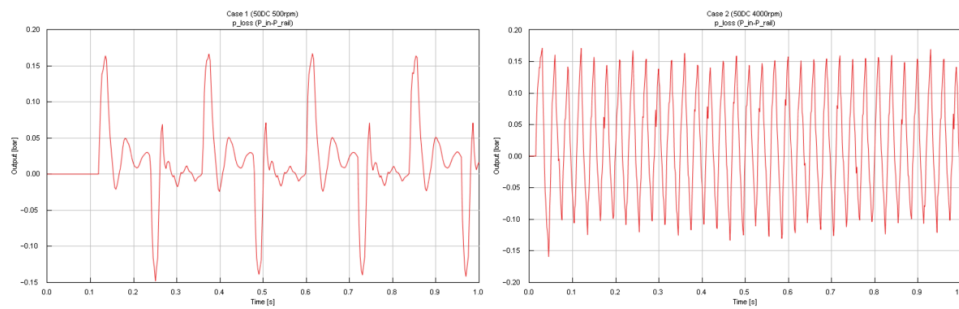


Figure 2.37 pressure loss in common rail i) 50 duty cycle of injector operation at 500 rpm ii) 50 duty cycle of injector operation at 4000 rpm

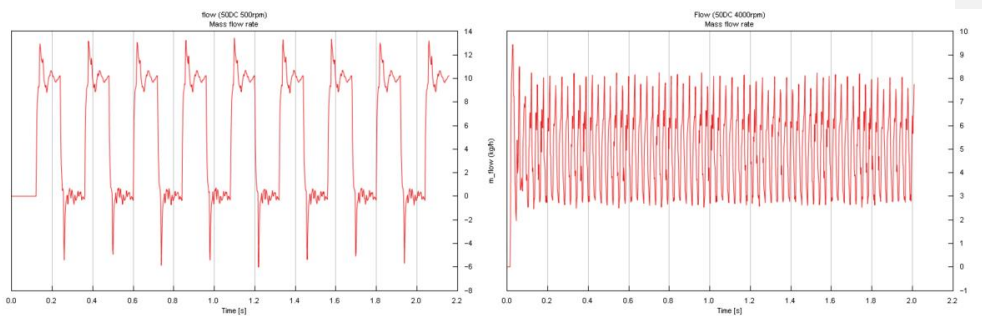
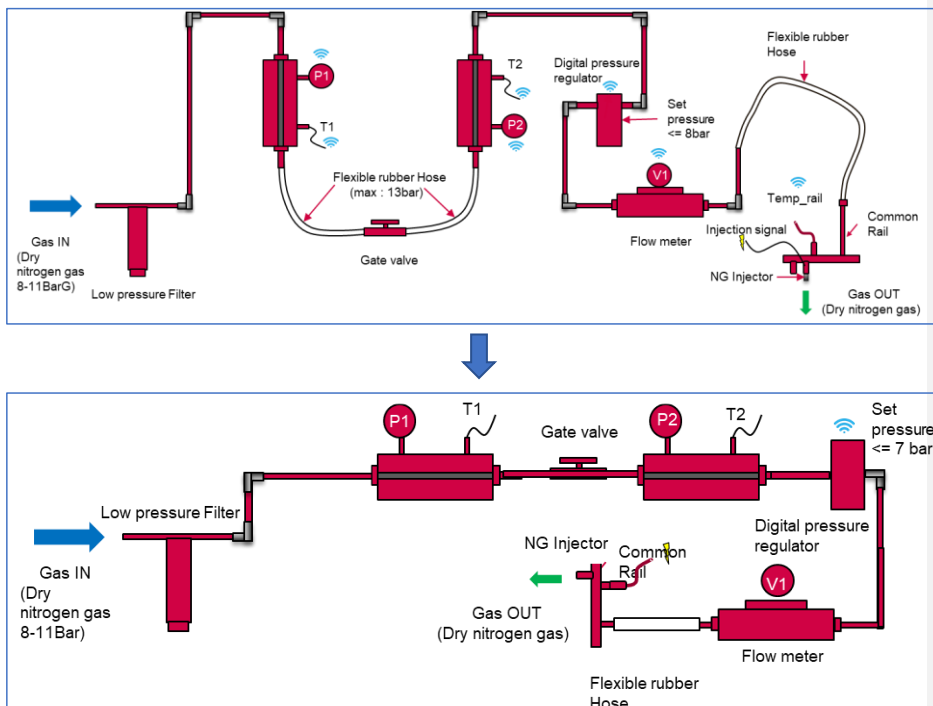


Figure 2.38 mass flow rate in common rail i) 50 duty cycle of injector operation at 500 rpm ii) 50 duty cycle of injector operation at 4000 rpm

Furthermore, improvements to reduce the error in the dynamic conditions (60-70-80) duty cycle are:

- **Reduce the length** of circuit
- **Avoid the Rubber/Nitrile connecting tube** since during pressure changes during the test conditions the walls are subject to expansion also damps the pressure waves which never happens in the vehicle circuit
- **The injector** must be still redefined for the dynamic testing conditions and add the **delay in actuation** to replicate the energizing time, so to match the dead time in the injection system to exactly predict the volume of gas injected per stroke. This parameter is very important for high-speed transient operations and low speed maneuver mitigation.
- The unwanted miter bends must be avoided as much as possible and keep the circuit as straight as possible
- In future the GT SUITE can be integrated with the bench via Simulink/Simscape so, data from bench used to train the model through neural training function in the GT SUITE, which acts similar to AI to predict the exact behavior of the system and improve the stability of the prediction

Comparison of current vs proposal bench layout is reported below.



2.4.4 Extensive Development

Run time dashboard setup: The run time dashboard is created to visualize the signals which acts very similar to the bench, so this acts as a digital twin of the bench. User Interface was created as simple as possible to make anyone in the test area to access and work easily on the GT SUITE.



Figure 2.40 Optimized Model of the Nozzle, Rail assembly and Pipe connections Fig. Real time dashboard created to easy analysis of run time data and compare while test bench is running in parallel

This enables the development of different layout and different test setups with out the involvement of the complex assembly and attachments in the real bench. Also allowing to sweep cases and conduct various studies which takes time to setup in the physical bench. Thus, this is considered as one of time reducing effort to study different case scenarios at least time, giving an edge in reducing physical, time, improving the work efficiency. This is one of significant milestone achieved during the development of the thesis.

3. Vehicle simulation

3.1 Description

The vehicle model was constructed based on the test bench model development approach, initially the simplified model was constructed to verify model behavior and to calibrate the pressure, mass flow characteristics. Once the stable model was constructed, we introduce the complex systems to the layout. Thus, it is easy identify the instability and fix the error while modelling which minimized the error and possible to identify and locate the pressure loss in the circuit. The calibration of the model required the data such as constant mass flow condition at the idle, transient, load conditions of the engine which was then introduced in the model to mitigate the same flow conditions in the vehicle. Thus, with updated model it was possible to predict the flow behavior and the pressure fluctuations in the real-world conditions. The steps involved reaching the final model of CNG model for vehicle was shown below in the below fig. we should not the same procedure was repeated again for the LNG vehicle model

The target of the analysis is to utilize the previous test bench circuit which was similar to the vehicle gas circuit cross section. The lab test bench was validated for the Nitrogen gas, now for the vehicle layout the validated pipes are taken with all the cross section and friction factors, the gas is replaced with the methane gas.

With the above changes the target was to accomplish the delta pressure measurement along the circuit. The same method of validation of the circuit was done taking in reference the data from the Engine bench.

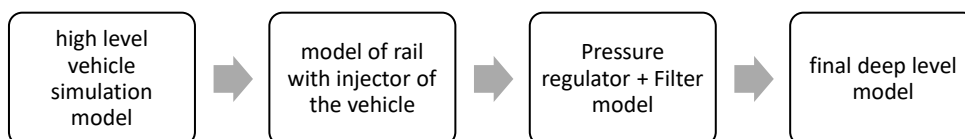


Fig.3. 1 flow chart representing the simulation procedure

3.2 CNG high level vehicle simulation

The model was developed was kept as simple as possible to minimize processing error. In the vehicle approach down stream the pressure regulator the model remains same for both the CNG layout and the LNG layout. But in the CNG due to high pressure difference the simulation failed due to instability in calculation due neighboring pipes have very high-pressure difference. This gave the deep insight regarding the Joule Thomson effect. When the neighboring pressure level was too high the gas reduces the temperature and starts freeze the components, the instability

is due to difference in temperature and density. This was over some by remodeling the circuit and input boundary conditions and temperature.

3.2.1 Boundary Condition

Gas	Methane
Quality	G20/G25
Temperature	23 °C (ambient)
Input pressure	Constant: Range 20 barg to 200 barg
output pressure to ambient atmosphere	0.3 barg
Solver	Explicit solver: Runge Kutta
Engine rpm variable	500 to 4000 rpm

Table 3. 1 CNG vehicle layout boundary conditions

3.2.2 Gas transport properties

Defining the proper gas at proper temperature is very important since this has adverse effect in the flow conditions in the circuit, the below vales are used for CNG vehicle model.

Carbon atoms per molecule	1
Hydrogen atoms per molecule	4
Lower heating value	5E007 J/kg
Critical temperature	190.4 K
Critical pressure	46 bar
Absolute entropy at 298 K	11618 J/kg-K
Dynamic viscosity	1.3 E-5 to 3.5E-5 kg/m-s
Thermal conductivity	0.03 to 0.2258 W/(m-K)

Table 3. 2 Gas transportation properties

3.2.3 Model description and layout

Components included in analysis are reported below. We can notice the common rail was considered as a simplified pipe of equivalent volume to keep the simulation effort simple. This was done at the development phase where the exact vehicle data was not available at this point. The simplified model was incorporated to design the pressure regulator where its design was complex behavior in controlling the pressure.

1. Straight pipes (stainless steel)
2. Orifices
3. Connectors, Flow splits and junctions
4. Pressure regulator
5. Flexible pipe and connector
6. Vehicle common Rail
7. Simplified model Gas injector (injector B)

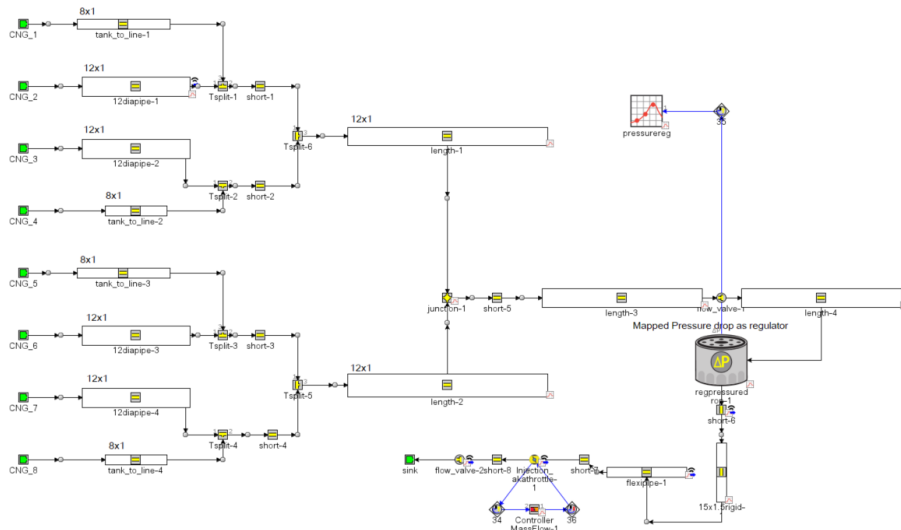


Fig.3. 2 First approximation model developed in GT SUITE to measure pressure loss and mass flow

To verify the model the input pressure to the circuit was given in 4 cases, thus we can measure the mass flow as expected in the intake manifold. It is also important to measure the behavior of the pressure control in pressure regulator which was modelled as a pressure drop where the important phenomenon of change in pressure, temperature have the influence in the density of the gas and flow behavior downstream the pressure regulator.

3.2.4 CNG high level simulation results

The study was realted to study the behaviour of the CNG flow condition and the behaviour in the outlet of the injector, thus the low value of 30 bar of tank pressure is taken as reference for low pressure (fuel) in the tank and the 220 bar was considered for high pressure (tank full) condition. The moderate values are considered such as 80 bar and 60 bar representing tank half filled. These are the input boundary pressure represents the output pressure of the cylinder at different pressure conditions, considering the tank full, half empty and low fuel conditions the simulation was carried out in 4 test cases as shown below:

input_boudrycondition						
Parameter	Unit	Description	Case 1	Case 2	Case 3	Case 4
Case On/Off		Check Box to Turn Case On	<input checked="" type="checkbox"/>	<input checked="" type="checkbox"/>	<input checked="" type="checkbox"/>	<input checked="" type="checkbox"/>
Case Label		Unique Text for Plot Legends				
cylinderpressure	bar	Pressure (Absolute)	220...	80...	60...	30...
temperature	C	Temperature	23...	23...	23...	23...

Fig.3. 3 input boundary condition

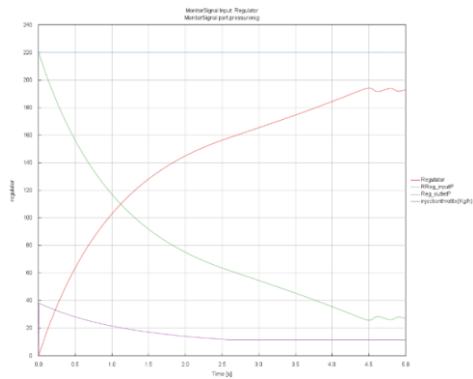


Fig 3.4 Input pressure 220 barg

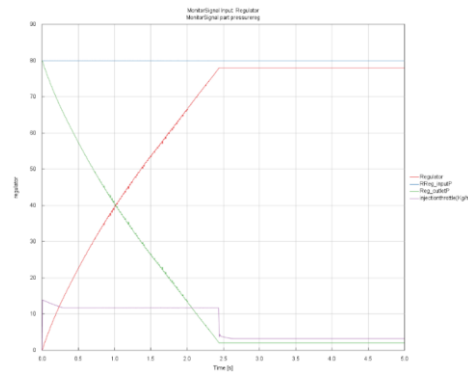


Fig 3.5 Input pressure 80 barg

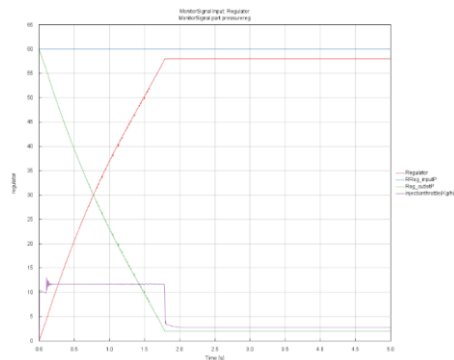


Fig 3.6 Input pressure 60 barg

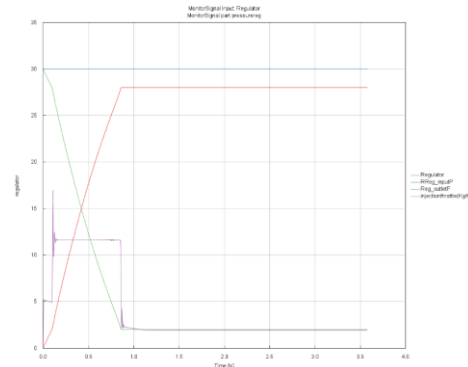


Fig 3.7 Input pressure 30 barg

The above results are verifying that the pressure regulator modelled was able to reduce the high pressure to low pressure, which requires to still reduce during the set pressure. The throttle (controller) at the end acts as 6-injector to maintain constant maximum mass flow rate of the injector B used in Engine. Model has no venturi or converging connections, thus the pressure loss calculated is 1st level approximation model. Pressure regulator model parameters are made as input as pressure loss in the circuit to reach the constant set pressure which was controlled downstream via throttle body to maintain the constant flow.

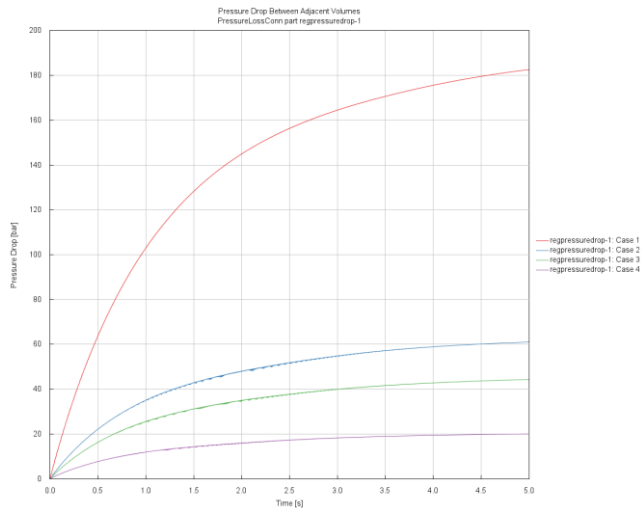


Fig.3.7 Pressure drop measured in the pressure regulator i) case 1 220 barg ii) case 2 80 barg iii) case 3 60 barg iv) case 4 30 barg

3.2.5 Joule-Thomson effect

The behavior of CNG gas at high pressure changes the flow behavior. Since the gas pass from high pressure to low pressure passing through the pressure regulator which was controlled by piston controlled by the spring action. This process the gas to cool down to sudden drop in temperature, which has worse effect when the temperature is in subzero, the components have possibility to freeze. This effect was realized in the GT SUITE model where we can notice there is sudden drop in the temperature due to Joule Thomson effect

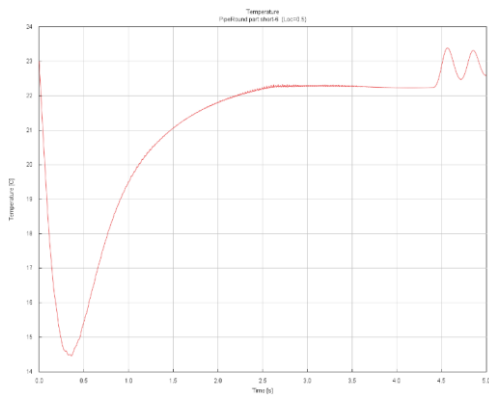


Fig.3. 8 input pressure 200 barg

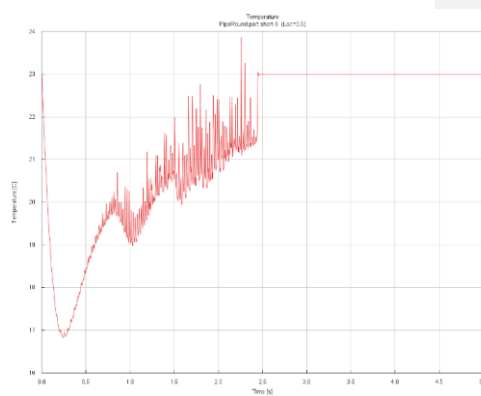


Fig.3. 9 input pressure 80 barg

The pressure measured during the low-pressure range recovered temperature faster than the high-pressure input, this indicates the more the time it takes to recover more the tendency to have the freezing of the component.

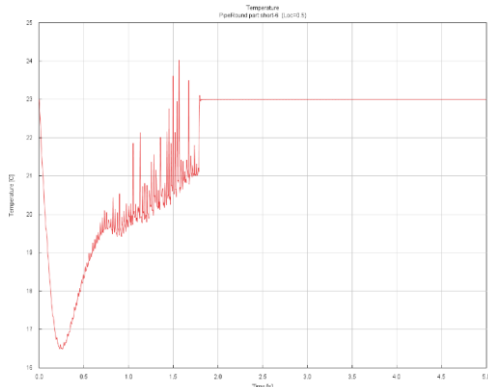


Fig.3. 10 Input pressure 60 barg

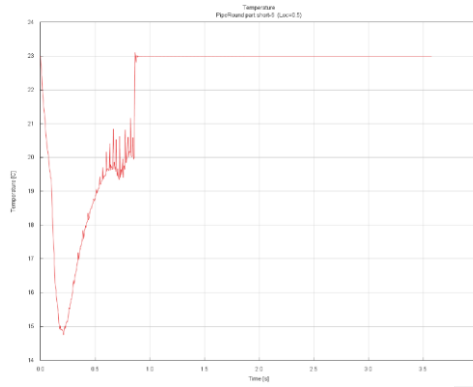


Fig.3. 11 Input pressure 30 barg

3.3 CNG deep level vehicle simulation

In order to the better and more deeper vehicle simulation, it was needed to model and integrate the rail and injector. The deep level simulation model was proceeded with exact pipe sections which are from the vehicle, which was already used in the previous model. The pressure regulator from the high-level model was more refined in the deep level simulation. In deep level analysis the model, the component sections are developed in the CAD in solidworks and then they are imported in the GEM 3D in GT SUITE and then 1D model was obtained which contains the exact model of the vehicle with volume splits and orifices, converging pipes sections. This process is important to reduce the percentage of error and to stabilize the model calculation.

3.3.1 Model description and layout

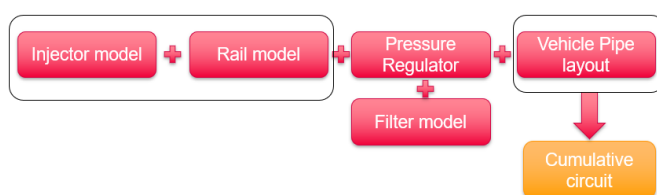


Fig.3. 12 Approach for the deep level vehicle model

As shown in the scheme, the modelling starts from the injector and combined with the rail. The CAD part file of the vehicle common rail and the injector was created, the 3D file was assembled and imported in the GEM 3D software to extract all exact volume to have the precise model.

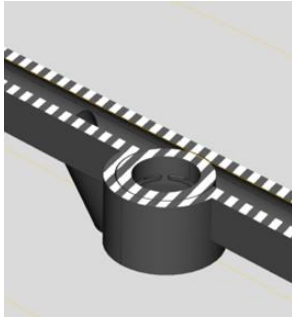


Fig.3. 14 Y-Y plane Internal geometry with injector B assembly with lid

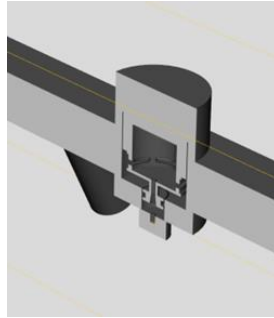


Fig.3. 15 In Z-Z plane Internal geometry with injector assembly with lids

The volume split was proceeded with the 1D pipe circuit which is used for the simulation. The model was sectioned with the simplified cross sections where the 3d components are converted into simplified volumes of tanks and variable pipe cross sections, which simplifies the model flow analysis compared to running large simulations in CFD software. Here you can note the sections are simplifies into sections of straight pipes and Split volume flows.

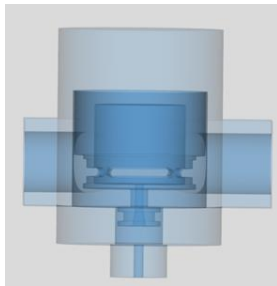


Fig.3. 16 Internal volume detection from the model



Fig.3. 17 : Internal volume converted as split flow

Unlike the previous lab test bench model this was complex since the Injector used was side feed, the pressure which will vary dynamically at all 6 injectors(Injector B) in different pattern based on the upstream/downstream delta P and also due to the design architecture of the injector location, this was noted during the simulation run time.

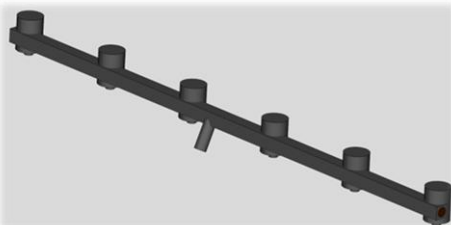


Fig.3.18. Rail solid model with simplified inlet connector

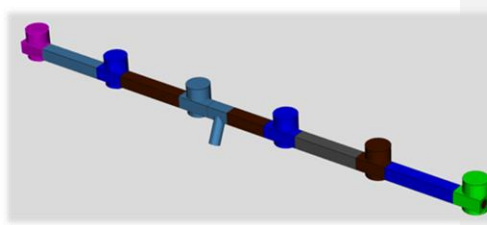


Fig.3. 19 Volume split and conversion procedure

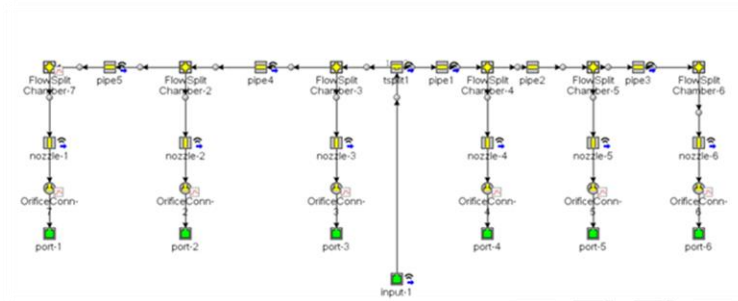


Fig.3. 2D Map of flow components of rail and injector imported and converted in GT SUITE model

This model represents complete model of the side feed injectors with the rail, the flow starts from input 1 where the pressure boundary conditions are given and the flow ends in the sink where the boundary conditions of the input manifold pressure was given. We can evaluate and tune the model for 100 duty cycle and then the tuning will be done and optimized for different input flow and pressure from the Engine bench data, which we can train the model for future prediction for different forward coefficient flow, thus we can simplify the complex model of the injector by eliminating the complex components such as armature coil, mass of the rod, offset conditions, lift profile for given current, which requires more data and fine tuning parameters for such complex systems

For simplified injector model described above the data required depends on the injector model chosen, for this reduce the complexity such as input current, data of armature, time delay for the lift, we considered the basic data of injector such as:

1. Opening and closing lift profile (simple model)
2. Opening and closing angles
3. Discharge coefficient of the injector at maximum needle lift (was calibrated from mass flow and pressure drop under steady state condition)

The input pressure was feed to the circuit which was designed to ramp with respect to the engine rpm, this allows to identify the closed result to match the supplier specification of the mass flow of the injector with the forward and reverse discharge coefficient which are obtained from the optimization and DOE obtained during development phase of this model.

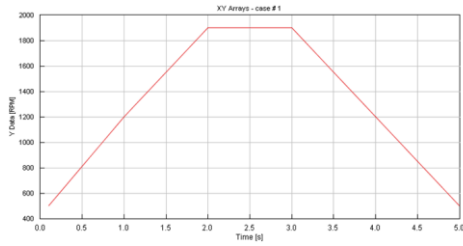


Fig. 3.21 Engine rpm vs Time

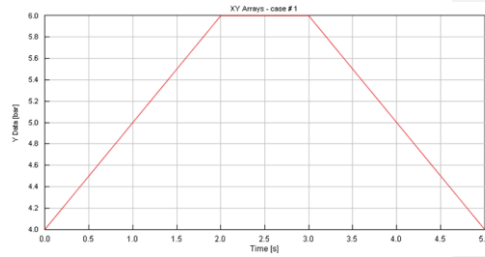


Fig. 3.22 Pressure input vs Time

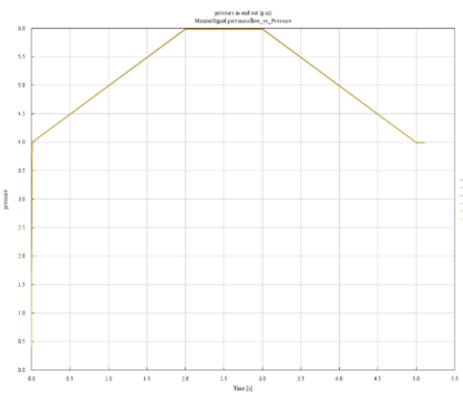


Fig. 3.33 Input pressure (profile)

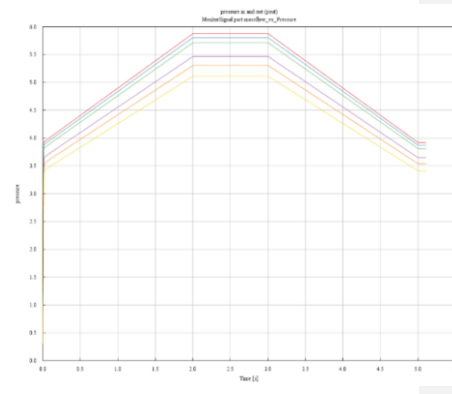


Fig. 3.34 Output pressure (barg)

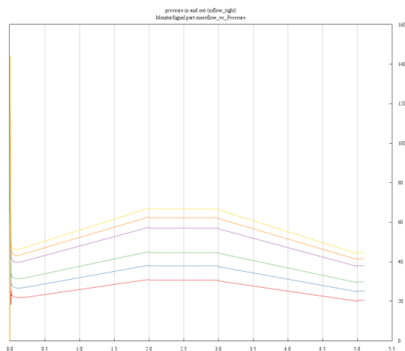


Fig. 3.35 Average mass flow rate in the rail (Kg/h) for discharge coefficients

From the above simulation, the injector B with the common rail was obtained which was very close to the vehicle output, since with the known data sets and raw data from the engine at certain operating range, it was possible to evaluate the mass flow and the pressure input which are primary data used for developing the model, the forward discharge coefficient was chosen considering the duty cycle of actual injector, but the exact map of the injector would make the model more robust.

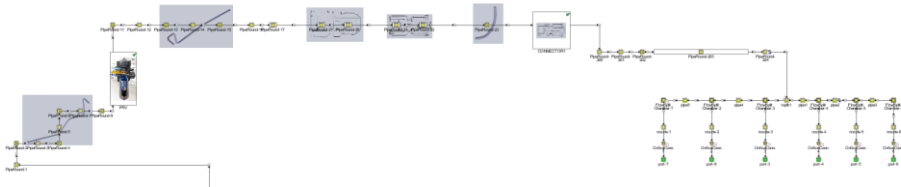


Fig.3. 36 Fuel line to common rail injection

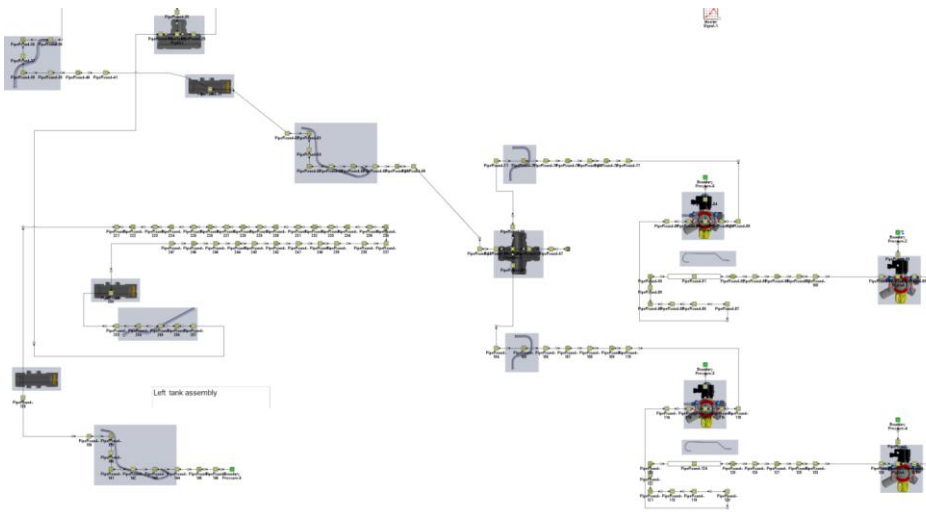


Fig.3.37 Accumulator (tank) to fuel line

3.3.2 CNG deep level test cases

The CNG deep level simulation was run at five different cases as mentioned in the below table.

Parameter	Unit	Description	Case 1	Case 2	Case 3	Case 4	Case 5
Case On/Off		Check Box to Turn Case On	<input checked="" type="checkbox"/>	<input checked="" type="checkbox"/>	<input checked="" type="checkbox"/>	<input checked="" type="checkbox"/>	<input checked="" type="checkbox"/>
Case Label		Unique Text for Plot Legends					
inputpressure	bar	Pressure (Absolute)	transientinput...	40	100	150	200
initialP_inircuit	bar	Initial Pressure in Circuit	0.3	0.3	0.3	0.3	0.3
temp_int	C	Temperature in circuit	23	23	23	23	23
RPM	RPM	Rotational Speed	1000	1000	1000	1000	1000
temp_inGAS	C	Temperature	23	23	23	23	23
WallTemp	C	Temp_internal rail	23	23	23	23	23
Temp	C	Imposed Wall Temperature	23	23	23	23	23
targetpressure_outreg		Target Rail Pressure [bar]	6	6	6	6	6
svdiameter		Output Signal Multiplier	2.25	2.25	2.25	2.25	2.25

Table 3. 3 test case setup

The below graph indicates the input pressure which was given to the system according to above tables (Case1 for transient and Case2 to Case5 for different pressure level).

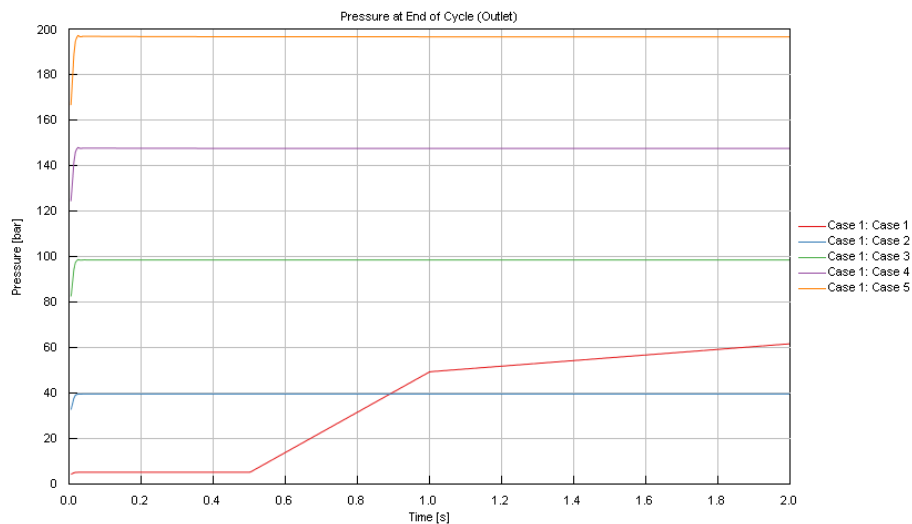


Fig.3.38 Pressure measurement at inlet pipe of the vehicle (round-85)

3.3.3 CNG deep level simulation results

3.3.3.1 Pressure regulator

The following figure indicates the calculated pressure downstream the pressure regulator, this proves that the regulator works by reducing high pressure from the input side to reduce or the safe operating set pressure level.

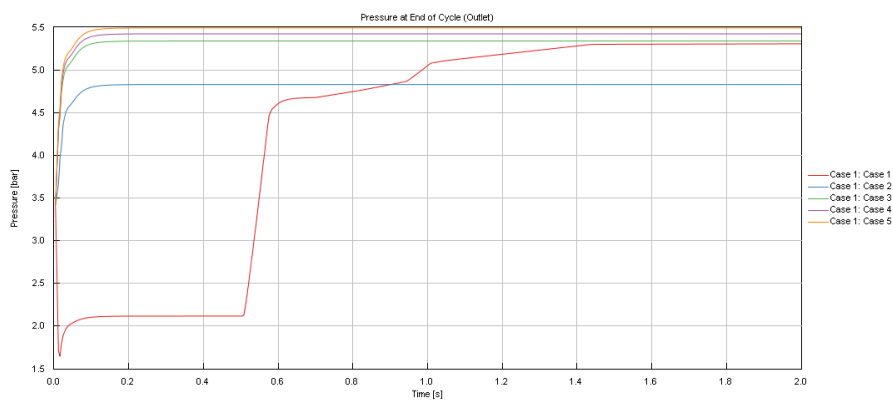


Fig.3.39 Pressure measurement downstream the pressure regulator

3.3.3.2 Rail

The graph below indicates the pressure measurement in the rail

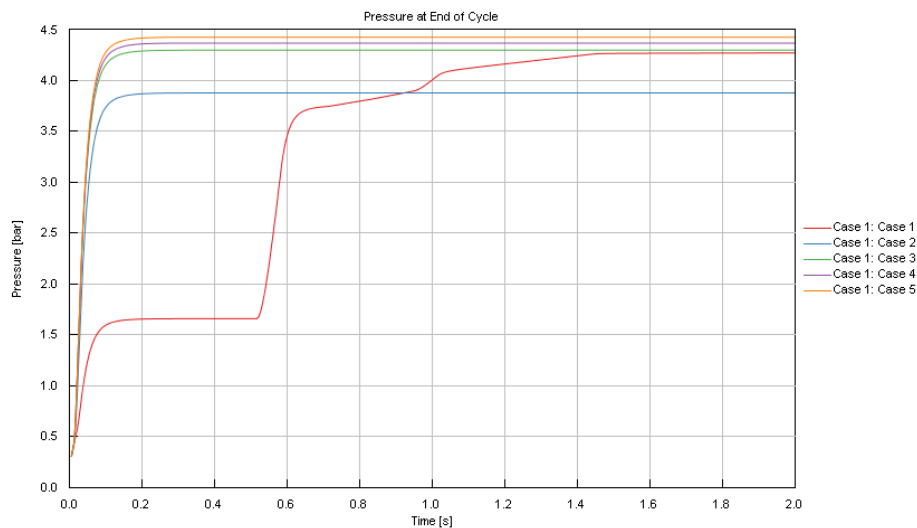


Fig.3. 40 pressure measurement in the rail

3.3.3.3 Mass flow

Once the pressure measurements are evaluated, we move to the mass flow measurements validated with engine test bench data. The mass flow was measured in the flex pipe where the pressure oscillations are reduced and also the results obtained a stable. These corresponds to the real flow results from the test bench; thus, this verifies the vehicle model is predicting very close to real world conditions.

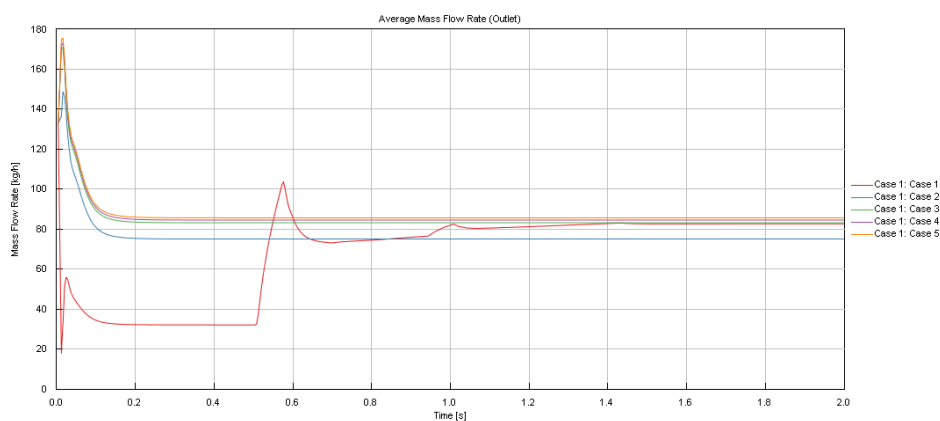


Fig.3.41 Mass flow measurement of CNG vehicle in flexipipe (from vehicle to rail)

3.3.4 Results at constant input and different engine rpm

The below graph indicates the constant pressure which was feed as input to the circuit from the tank to check the pressure and mass flow behavior at different engine rpm to verify the model capability to show the pressure loss.

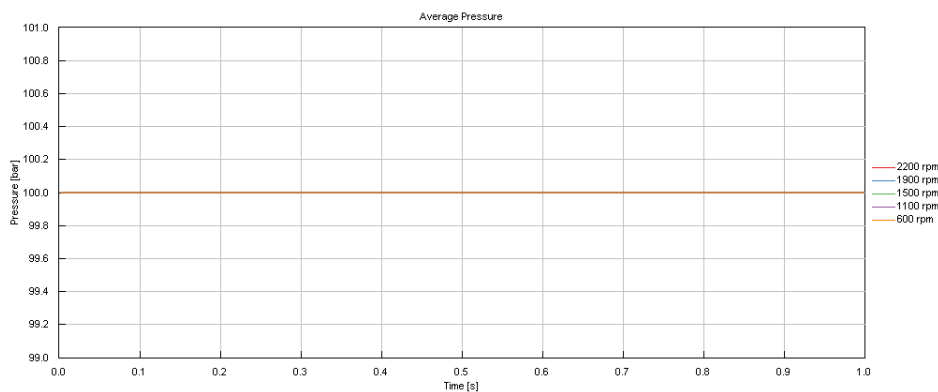


Fig.3.42- Input pressure from the CNG storage tank (accumulator)

3.3.4.1 Pressure measurement in pipe

The graph represents the pressure variation which was observed in the flex pipe which connects from pressure regulator to the common rail during the different flow conditions of the injector which operate at different duty cycle

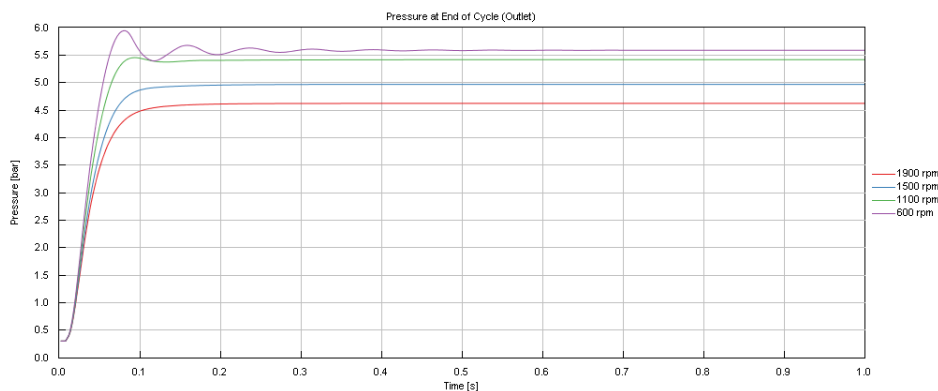


Fig.3. 43 Pressure measurement in flex pipe of the vehicle layout at different rpm

3.3.4.2 Rail

The below graph denotes the pressure measured in the fuel rail at different flow conditions of the injector which operate at different engine rpm.

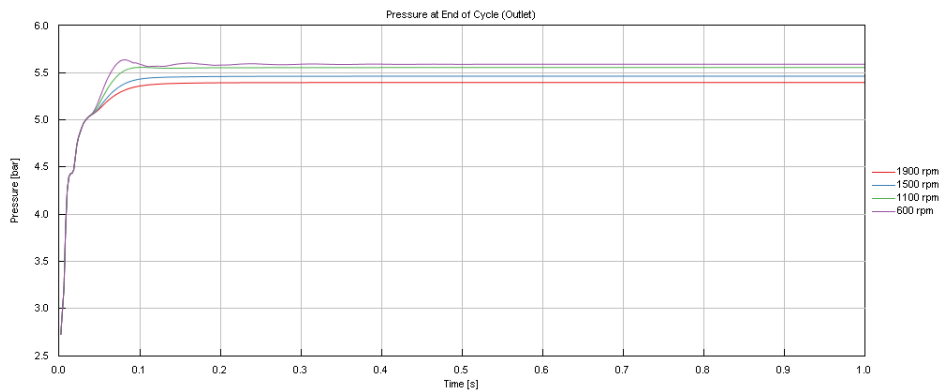


Fig.3. 44 Pressure measured in the fuel rail at different flow conditions

Looking at mass flow rate in the rail, it is calculated **58.48 kg/h** at 1400rpm versus the **60.64 kg/h** measured and resulting in average **3.56% error**.

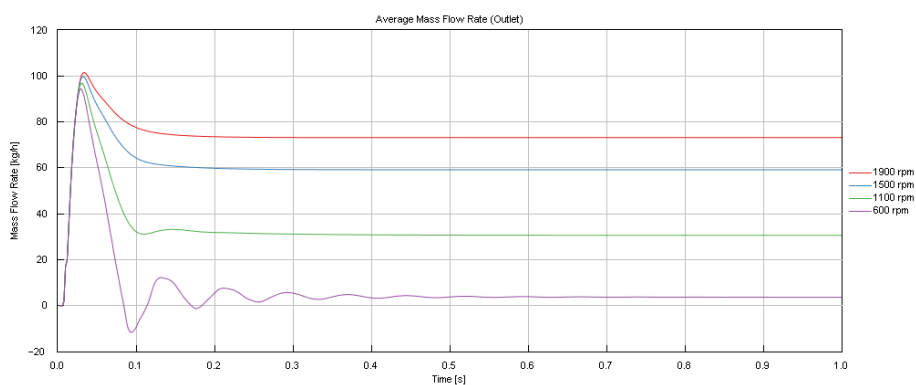


Fig.3. 45 mass flow rate measured in the rail at different engine rpm

3.3.4.3 Temperature measurements at pressure regulator

The graph below represents the temperature changes upstream pressure regulator which was captured during the simulation. It can be noticed that the gas temperature was low.

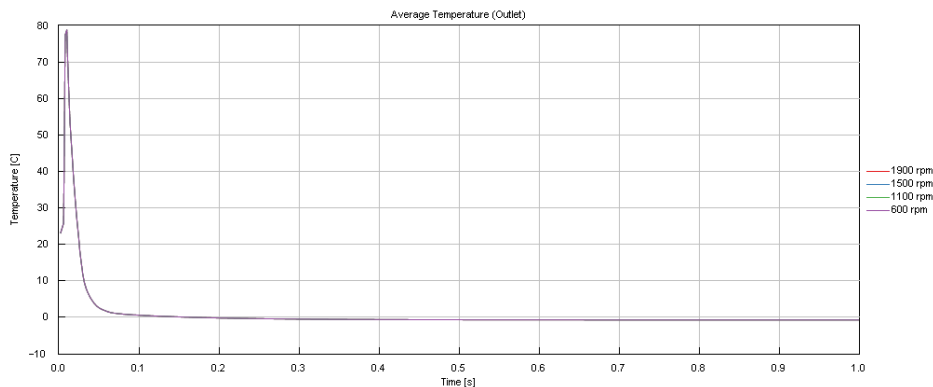


Fig.3. 46 average temperature measured at input of the pipe from the tank

Looking downstream pressure regulator as reported on below chart, we can notice the temperature has been slightly increased from the low temperature to the ambient temperature thanks to the temperature exchanger which was inbuilt in the pressure regulator to increase the temperature of the gas. since the gas passes through the orifices at high pressure to low pressure the cooling occurs, this process avoids the freezing of the components, the same was observed in the simulation, which indicates the model capability to mitigate the gas flow in vehicle in the real world conditions.

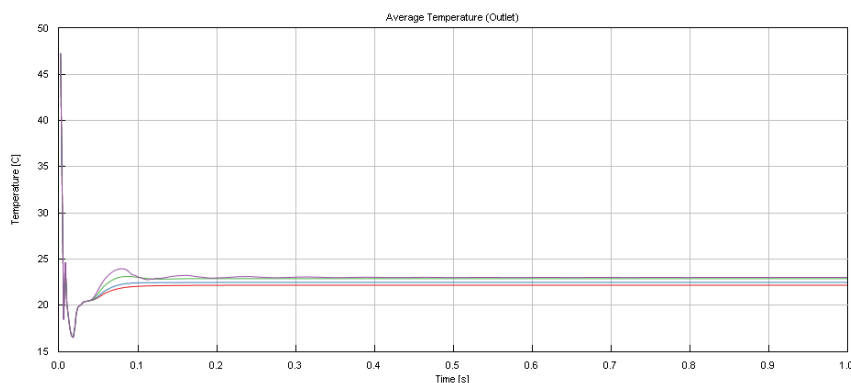


Fig.3. 47 Average temperature measured downstream of the pressure regulator

3.3.4.4 Density variation

The below graph represents the density variation observed at the upstream pressure regulator, which remains almost same since the temperature of the gas almost remains the same throughout all operating points.

Commented [SK(G1):

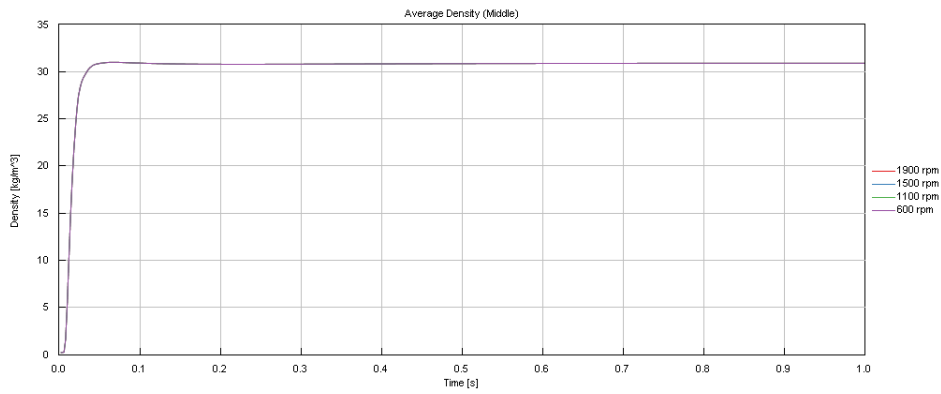


Fig.3. 48 Density variation observed at the upstream pressure regulator

On the other hand, downstream pressure regulator, density variation is observed due to the changes in the temperature.

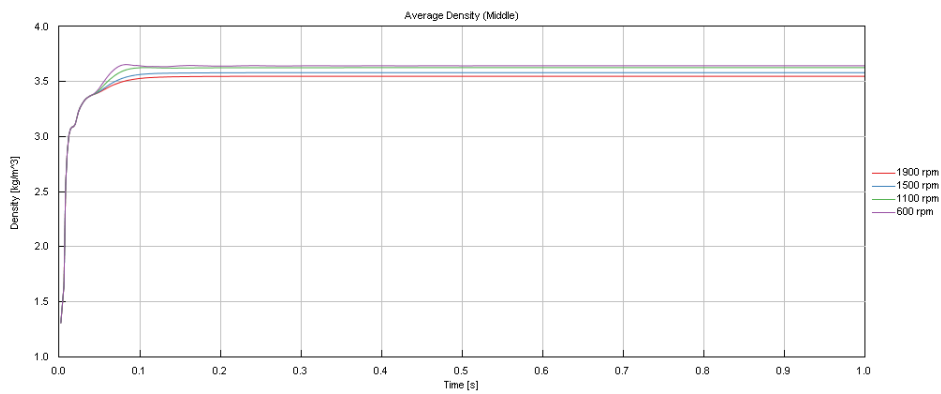


Fig.3. 49 density variation is observed downstream pressure regulator

Finally, looking at mid-section of the rail as reported in the following chart, we can notice also density variation

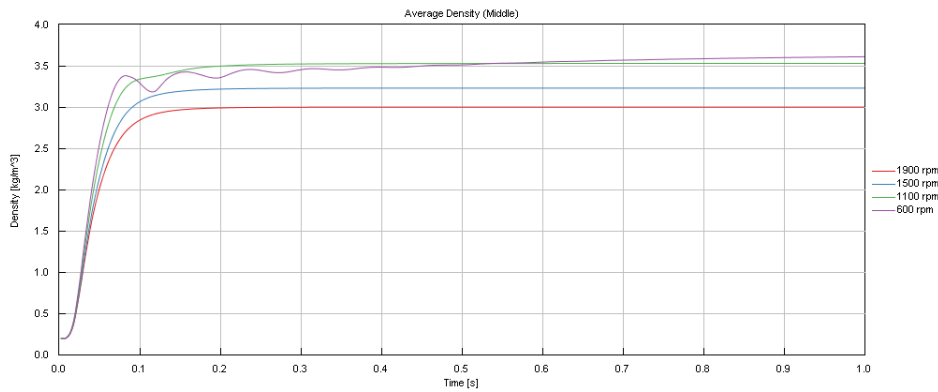


Fig.3. 10 Average density measured in the rail

3.4.2 Pressure loss analysis of different cross section

For further analysis the complete vehicle layout was introduced with increased pipe cross section to analysis of the pressure changes, this was carried out a step to analyze if there are any changes in improving vehicle circuit to reduce the pressure loss

The below table represents the case setup, choosing 1100 rpm and 33.43% duty cycle of injector for the simulation, since I have the known output of the values.

Main							
Parameter	Unit	Description	Case 1	Case 2	Case 3	Case 4	Case 5
Case On/Off		Check Box to Turn Case On	<input checked="" type="checkbox"/>	<input checked="" type="checkbox"/>	<input checked="" type="checkbox"/>	<input checked="" type="checkbox"/>	<input checked="" type="checkbox"/>
Case Label		Unique Text for Plot Legends	dia 10	dia 11	dia 12	dia 13	dia 14
inputpressure	bar	Pressure (Absolute)	100	100	100	100	100
initialP_inCircuit	bar	Initial Pressure in Circuit	0.3	0.3	0.3	0.3	0.3
temp_int	C	Temperature in circuit	23	23	23	23	23
RPM	RPM	Rotational Speed	1100	1100	1100	1100	1100
temp_inGAS	C	Temperature	23	23	23	23	23
WallTemp	C	Temp_internal rail	23	23	23	23	23
Temp	C	Imposed Wall Temperature	23	23	23	23	23
holeDiameter	mm	Hole Diameter	4.68	4.68	4.68	4.68	4.68
dutycycle	percentage		33.43	33.43	33.43	33.43	33.43
DIA	mm	Diameter at Inlet End	10	11	12	13	14

Fig.3. 11 case setup used for simulation

Input : The below chart represents the input pressure measured at the inlet of the circuit

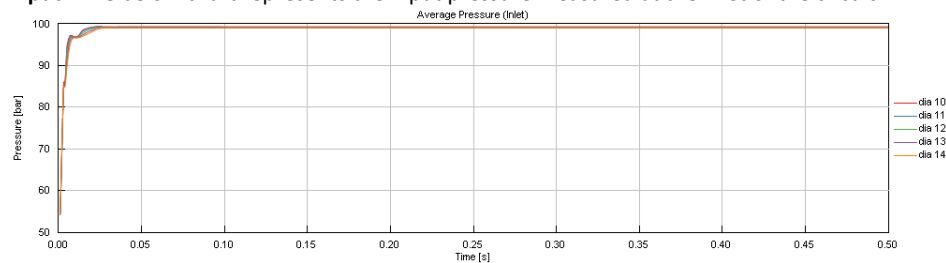


Fig.3. 12 Input pressure measured at the inlet of circuit

T-Junction of the left and right tank:

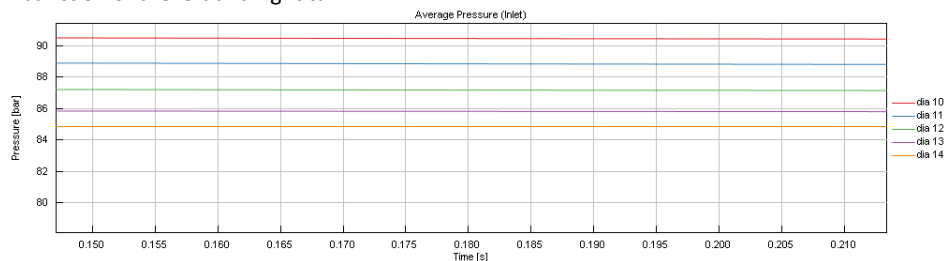


Fig.3. 13 the pressure measured at the T junction connecting the two CNG tanks in the vehicle

Upstream PRV

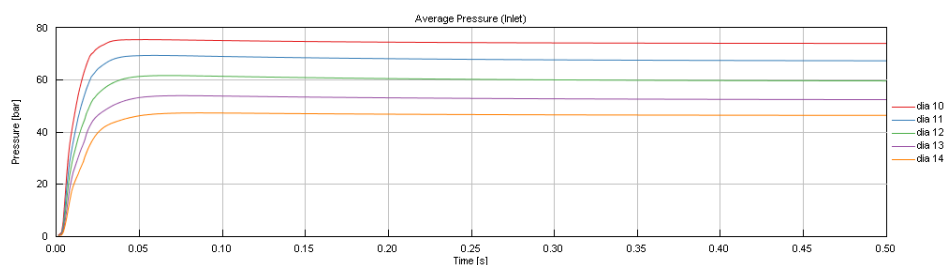


Fig.3. 14 Pressure measured at the upstream of the pressure regulator

Downstream PRV

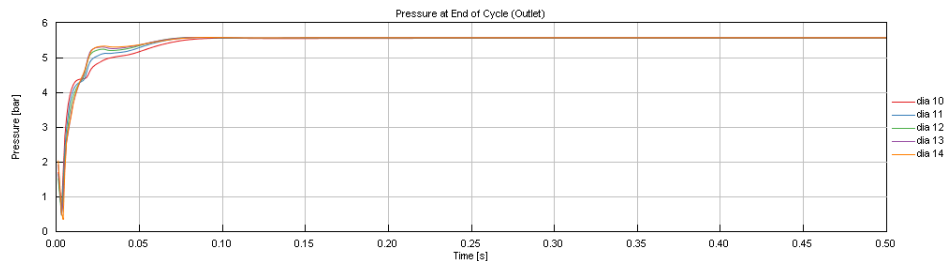


Fig.3. 15 Pressure measured at the downstream of pressure regulator

Rail

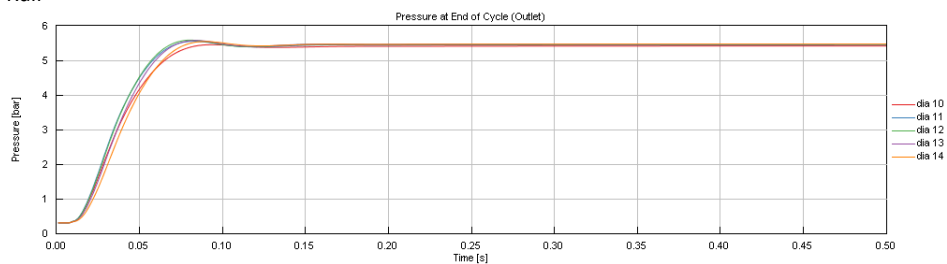


Fig.3. 16 Pressure measured at the rail

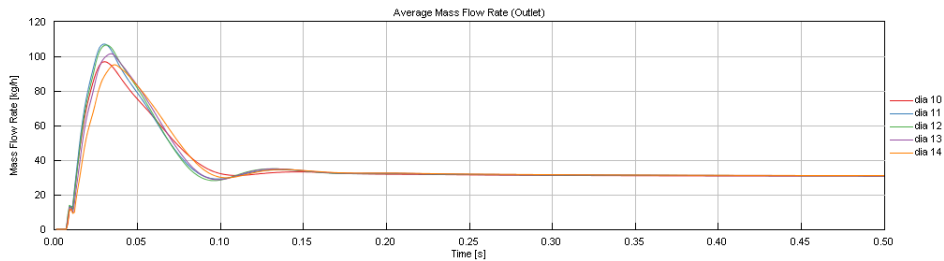


Fig.3. 17 Mass flow rate measured in the rail

Here we can note that the injector flow was matched with the simulation values which are close to specs at 20°C that flow rate was 24.5 kg/h maintaining rail pressure of 5.5 bar which was with close tolerance of $\pm 2\%$ error tolerance.

Which specifies that the model was able to replicate the real time data coming from the bench, which is close to the vehicle data.

Average temperature in rail:

The below graph represents the average temperature which was observed in rail when different vehicle pipe diameters are chosen, irrespective of the changes in the diameter, the temperature in unaffected thus the density

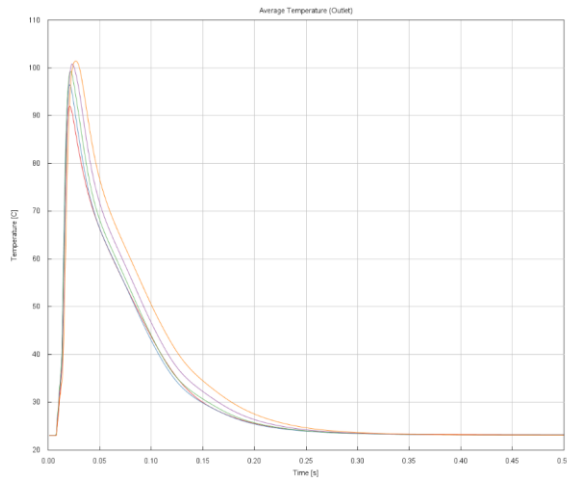


Fig.3. 18 Average temperature measured in the rail

Realtime plots : (monitored signals) (diameter 10mm)

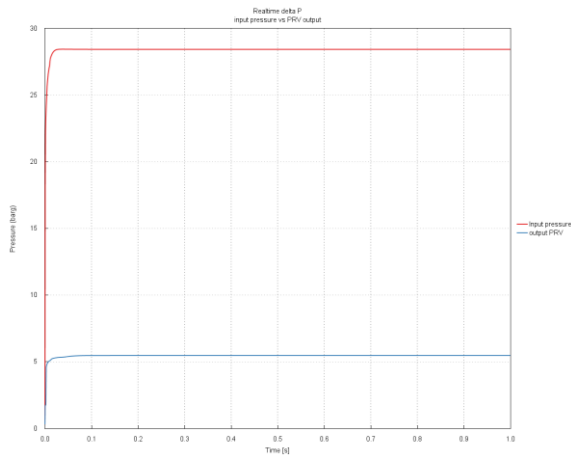


Fig.3. 20 Real time input pressure and output pressure regulated at output at 10 mm diameter of the circuit connection

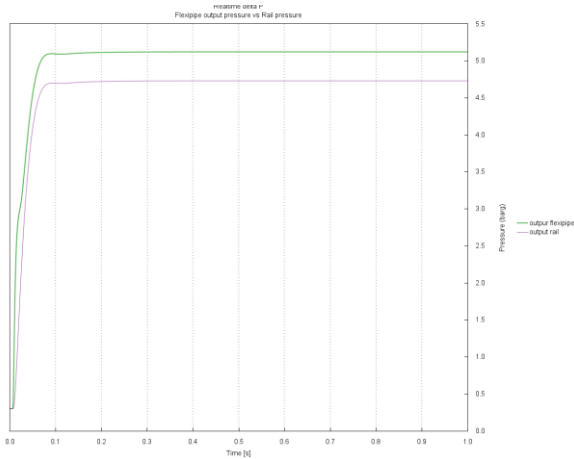


Fig.3. 19 real time measurement of the pressure from the flexipipe and the rail

the above graph was obtained during the simulation, which was recorded during the run time, which represents the pressure measurement from the input pressure regulator and output of the pressure regulator with the vehicle layout diameter change of 10 mm and the second figure represents the pressure measurement in the flex pipe and in the common rail

This simulation proves that even when we change diameter of the entire circuit the behavior of the pressure regulator plays important role, there are changes occurring upstream pressure regulator, but downstream the pressure regulator we can observe the pressure loss is more, thus improving the pipe diameter post the pressure regulator will be cost effective solution.

3.4 LNG high level vehicle simulation

3.4.1 Boundary condition:

The model was developed was kept as simple as possible to minimize processing error. In the vehicle approach downstream the pressure regulator model was developed as a pressure loss table with lookup function, since this data was available from the supplier. Unlike the CNG vehicle, there are not much difference in temperature and density since the pressure was low in this system.

Gas	Methane
Quality	G20/G25
Temperature	23 °C (ambient)
Input pressure	Range 5 barg to 40 barg (actual working max 20barg)
output pressure to ambient atmosphere	0.3 barg
Solver	Explicit solver: Runge Kutta
Engine rpm variable	500 to 4000 rpm

Table 3. 4 Boundary conditions of high level CNG vehicle layout simulation

3.4.2 Model description and layout

The vehicle layout was built in the CAD software and then the cad was imported in GEM3d software of GT SUITE, then the extract volume feature was utilized to convert the volume features into 1D flow pipe circuit. The similar process was done for the LNG circuit, the tunned model

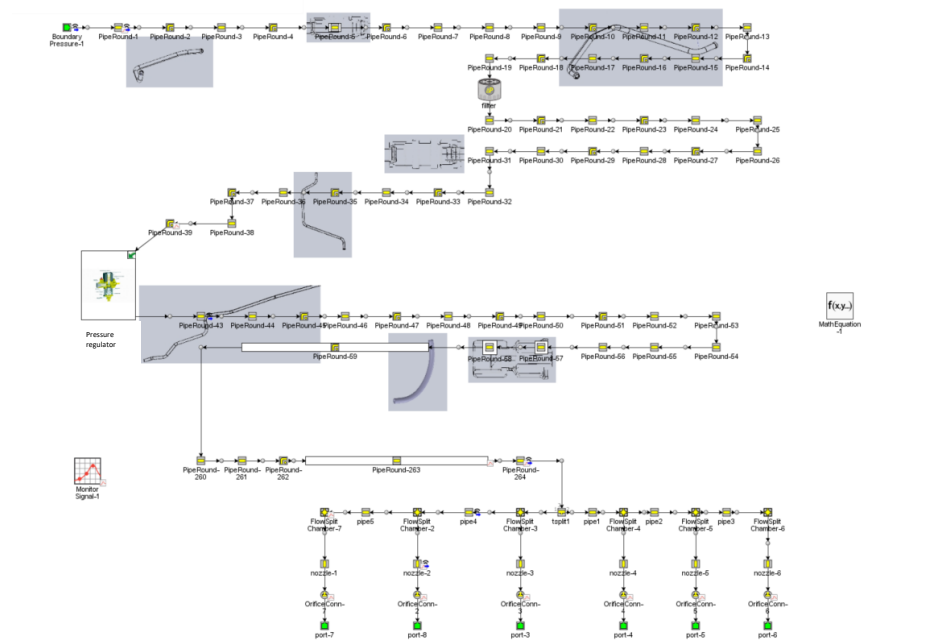


Fig.3. 21 Complete vehicle layout used in LNG high level vehicle simulation

which was already used in the CNG system , the Common rail and the injector system is utilized. The downstream LNG and CNG the pipe system and the components are similar.

3.4.3 LNG high level simulation results

The model was checked with the boundary conditions, where the fuel transport properties of the methane was utilized, which was already discussed in the CNG high level model description, the input pressure to the circuit was given as a ramp to check the validation of the circuit, since the data from the engine at specific points where they are operated during the steady state conditions had the steady flow in the fuel, these are the data utilized to calibrate the model-

From the below figure we can notice the pressure regulator output pressure, flex pipe output pressure, rail pressure and input pressure, which plotted on the same graph for the ease of readability, the Realtime data which are measured during the simulation. Since there are no high pressure in the system, the implicit solver was used to reduce the calculation period and extensive steady for 10s was obtained. This gave the edge to compare with the engine results and relate with the vehicle.

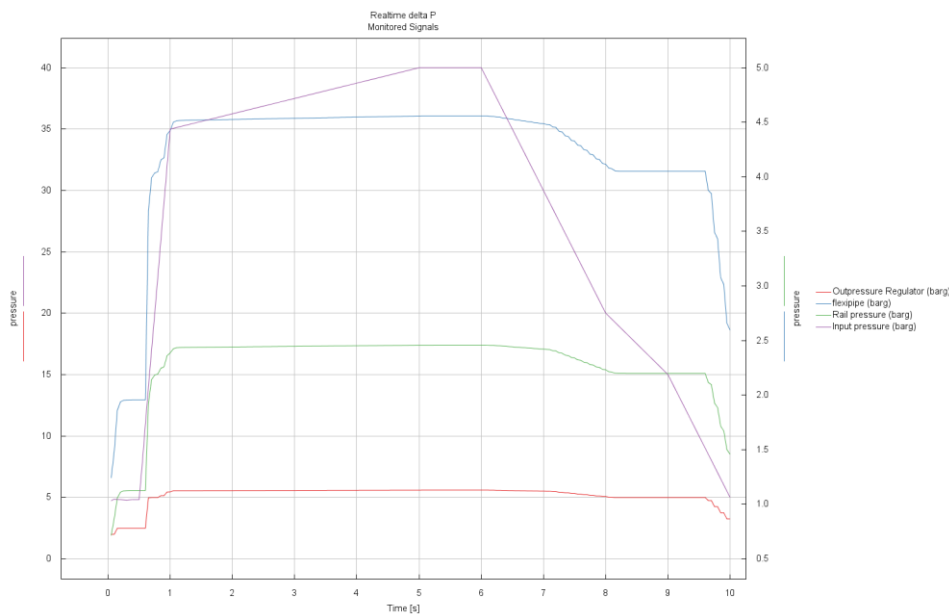


Fig.3. 22 Pressure signals monitored in output of pressure at input pipe, regulator, connecting Pipe and Rail

Pressure regulator downstream (total pressure loss):

The pressure regulator output was measured as total pressure loss, since this pressure loss is directly proportional to the pressure reduction function, when the input pressure was given more than 5 barg, the pressure should be always reduced, and the free flow starts if the pressure is equal to the set pressure this condition is called permeability , if the pressure was higher than set pressure by the supplier, then the pressure will be reduced to set pressure levels, but this stepping down behavior response time varies depending on the transient

condition, the model validated was working for slow transient response., the sudden high response cause instability , also sudden high transition almost never occurs in vehicle behavior . the below graph represents the pressure reduced in the pressure regulator for the input given

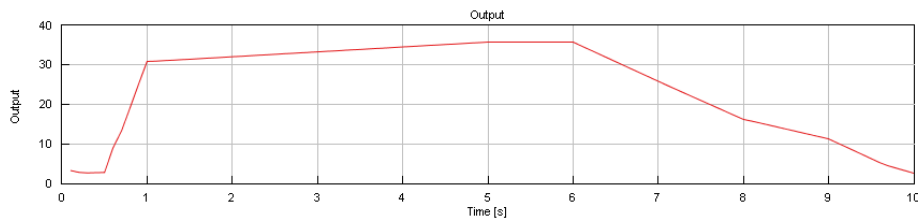


Fig.3. 23 Total pressure measured downstream the pressure regulator

3.5 LNG deep level Vehicle layout

The high level simulation model was used here, in the previous high level simulation we gave the different input pressure and measured the pressure loss, but to take the simulation to the real world conditions, the model was subjected to different engine rpm to mitigate the different flow behavior in the circuit. The corresponding duty cycle was known from the calculation from the injection quantity and the flow conditions coming from the engine test bench, this was important parameter introduced to close the error gap and to increase the robustness of the simulation results

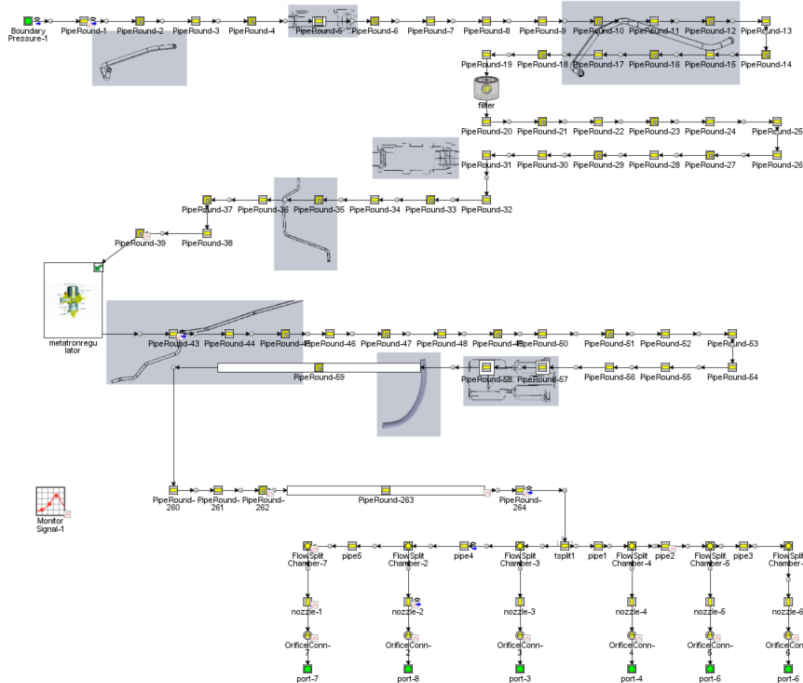


Fig.3. 24 Complete vehicle layout used in LNG high level vehicle simulation

The below table show test case setup used for the simulation. Here we should notice that the input pressure was given as 30 bar which was higher but in actual condition the pressure was 20 bar and we can notice the duty cycle varies for each engine running condition.

Case On/Off	Check Box to Turn Case On	<input checked="" type="checkbox"/>	<input checked="" type="checkbox"/>	<input checked="" type="checkbox"/>	<input checked="" type="checkbox"/>	<input checked="" type="checkbox"/>
Case Label	Unique Text for Plot Legends	1800 rpm	1500 rpm	1300 rpm	1000 rpm	594 rpm
flowgradient	bar/(L/min)	0.3	0.3	0.3	0.3	0.3
volumeflow	L/min	0.3	0.3	0.3	0.3	0.3
corrspresuredrop	bar	20	20	20	20	20
crackingspdrop	bar					
initialP_incircuit	bar	0.3	0.3	0.3	0.3	0.3
temp_int	C	23	23	23	23	23
WallTemp	C	23	23	23	23	23
Temp	C	23	23	23	23	23
dutycycle	duty cycle in percentage	46	42	36	27	10
holediameter	mm	4.68	4.68	4.68	4.68	4.68
rpm	RPM	1800	1500	1300	1000	549
input	bar	30	30	30	30	30

Fig.3. 25 case setup for the deep level simulation

3.5.1 LNG vehicle simulation deep level results:

3.5.1.1 Pressure in filter

The below graph indicates the pressure which was measured downstream the filter which was found upstream the pressure regulator (round pipe 20)

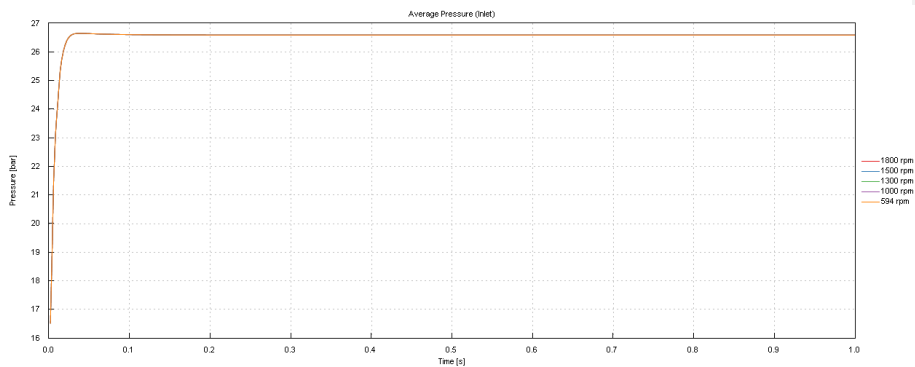


Fig.3. 26 Pressure measured at round pipe-20 at different engine rpm

3.1.5.2 Pressure drop in Filter:

The below figure represents the pressure drop in the filter which was obtained from the adjacent pipe pressure, the drop was measured 1.0 bar irrespective the mass flow at different rpm.

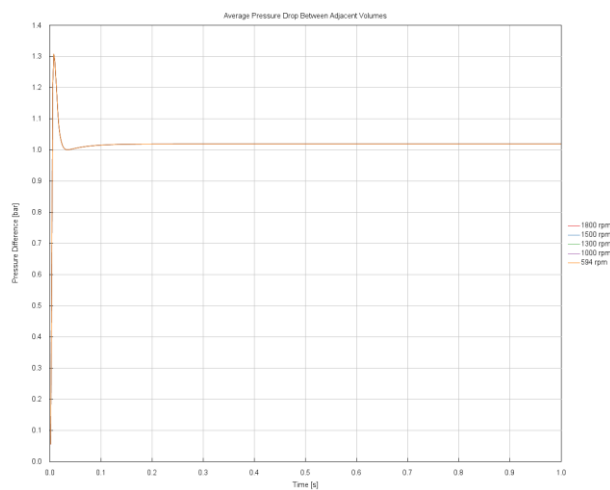


Fig.3. 27 Pressure drop measured in teh filter at different engine rpm

3.1.5.3. Pressure regulator

The pressure measured downstream the pressure regulator was reported below, the pressure difference was observed at different engine operating condition

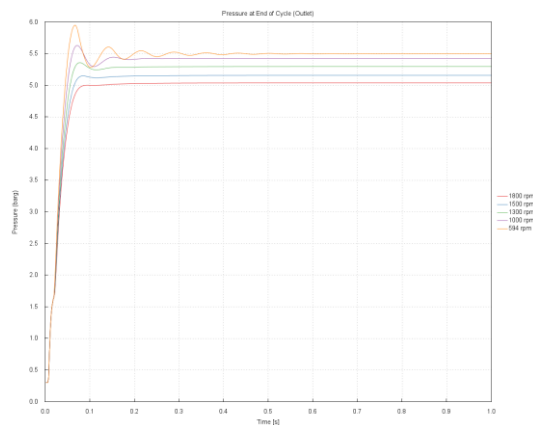


Fig.3. 28 The pressure measured downstream the pressure regulator

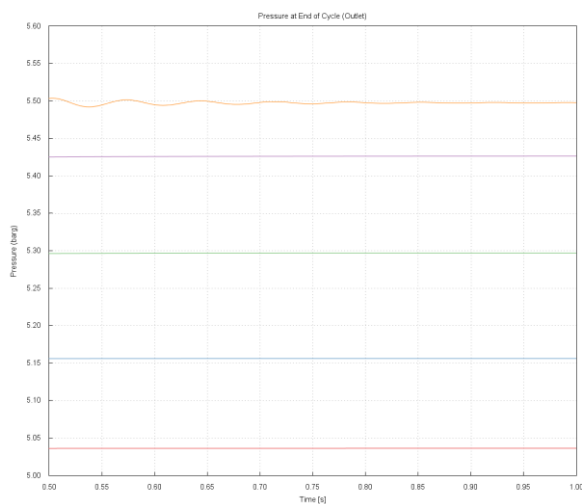


Fig.3. 29 magnified view of The pressure measured downstream the pressure regulator

3.1.5.4 Rail pressure

The below graph denotes the pressure measured in the fuel rail at different flow conditions of the injector which operate at different engine rpm.

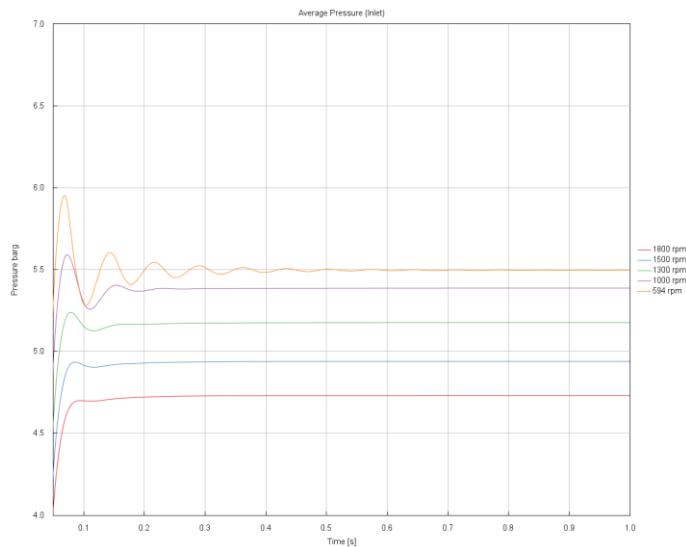


Fig.3. 30 Average pressure measured in the fuel rail at different engine rpm.

3.1.5.5 Rail temperature

The below graph denotes the temperature readings measured in the fuel rail at different flow conditions of the injector which operate at different engine rpm. Here we can notice the temperature spikes, these are normal over estimation (noise) since we used the Explicit simulation, it captures the high frequency signals, this peak is due to the sudden flow in circuit caused high pressure difference then it converges after 0.5s in the simulation.

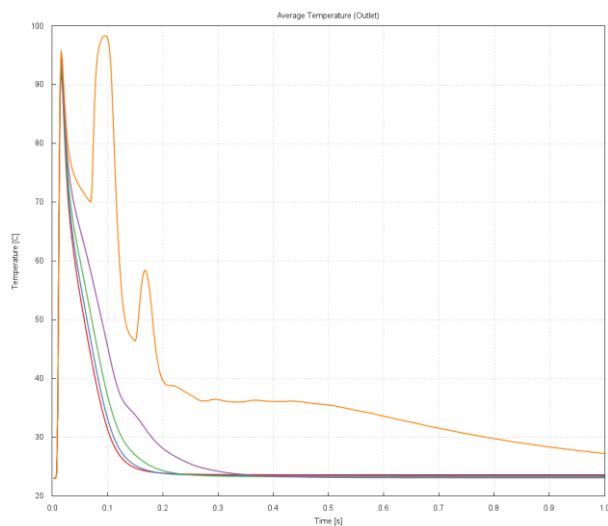


Fig.3. 31 Temperature measured in the rail at different engine rpm.

3.1.5.6 Density variation

The below graph represents the density variation observed at the upstream pressure regulator, which remains almost same even though there are slight temperature change in the gas, but the density remains same unlike in the CNG system, thus LNG has less fluctuations in general compared to the CNG circuit.

Commented [SK(G2):

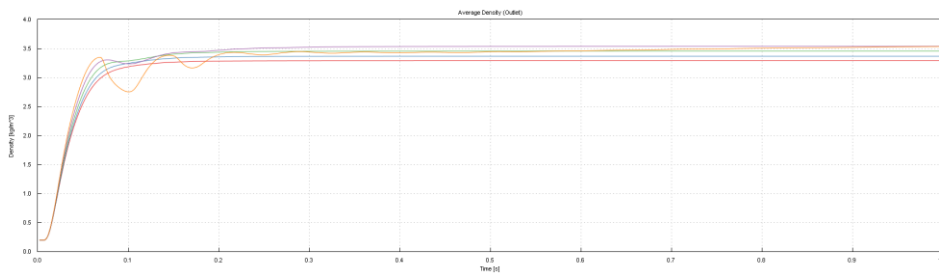


Fig.3. 32 Density variation observed at the upstream pressure regulator

3.6.1 Pressure loss analysis of different cross section of pipe:

For further analysis the complete vehicle layout was introduced with increased pipe cross section to analysis of the pressure changes, this was carried out a step to analyse if there are any changes in improving vehicle circuit to reduce the pressure loss

Parameter	Unit	Description	Case 1	Case 2	Case 3	Case 4	Case 5
Case On/Off		Check Box to Turn Case On	<input checked="" type="checkbox"/>	<input checked="" type="checkbox"/>	<input checked="" type="checkbox"/>	<input checked="" type="checkbox"/>	<input checked="" type="checkbox"/>
Case Label		Unique Text for Plot Legends	8mm diameter	10mm diameter	12mm diameter	13mm diameter	14mm diameter
input	bar	Pressure (Absolute)	30	30	30	30	30
dia	mm	Diameter at Inlet End	8	10	12	13	14
volumeflow	L/min	Characteristic Volume Flow	0.3	0.3	0.3	0.3	0.3
initialP_inicircuit	bar	Initial Pressure in Circuit	0.3	0.3	0.3	0.3	0.3
temp_int	C	Temperature in circuit	23	23	23	23	23
WallTemp	C	Temp_internal rail	23	23	23	23	23
Temp	C	Imposed Wall Temperature	23	23	23	23	23
dutycycle		duty cycle in percentage	42	42	42	42	42
holediameter	mm	Hole Diameter injector	4.68	4.68	4.68	4.68	4.68
rpm	RPM	Rotational Speed	1500	1500	1500	1500	1500
corrspresuredrop	bar						
flowgradient	bar/(L/min)	Flow Rate Gradient	0.3	0.3	0.3	0.3	0.3
crackingdrop	bar						

Fig.3. 33 test case setup for the cross section sweep study to analyse pressure loss differences

Inlet pressure :

The input pressure of the LNG circuit was kept at the constant pressure of 30 bar, the steady flow was used to observe the pressure loss at different diameter of the pipe which are taken in 5 test cases.

Downstream Filter:

The steady state pressure when passed through the filter passing the pipe system produced varied pressure loss down stream the filter, this is due to the membrane behaviour of the filter and this was obtained from the filter model which was completely build based on the supplier

data and constructed a look up table , which take the loss coefficient and calculates, the calculated values are matching the simulation results.

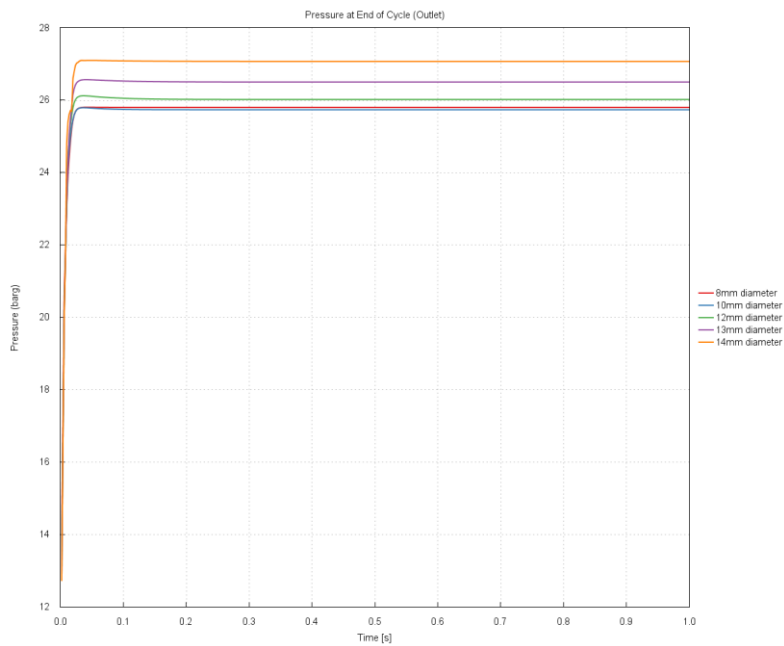


Fig.3. 34 Pressure measured downstream filter at different cross section of the pipe at the same location

Pressure regulator:

The below graph represents the pressure measured upstream the pressure regulator we can notice there are changes in the pressure where the pressure drop is maximum at the low diameter pipe and the pressure loss observed minimum at 14mm diameter pipe

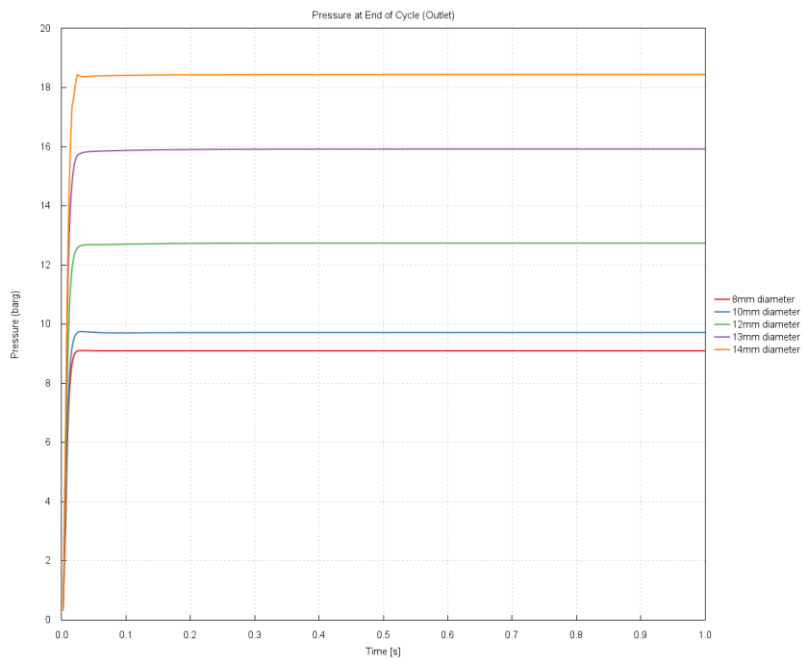


Fig.3. 35 Pressure measured upstream pressure regulator at different cross section of the pipes at the same location

Flexipipe:

Below graph was the pressure measurement of the circuit in the flexipipe which was connecting pipe downstream pressure regulator and the upstream rail

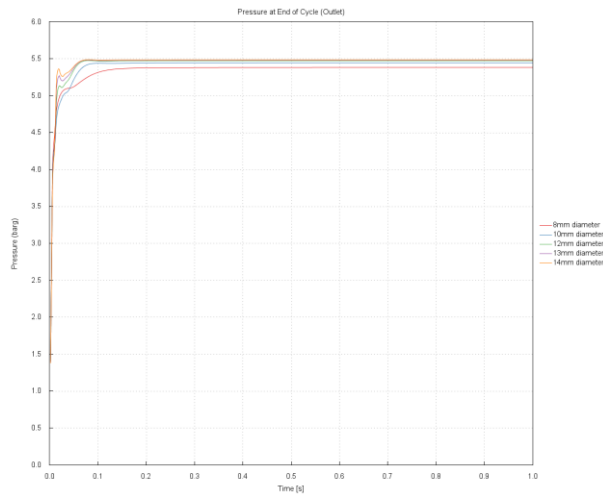


Fig.3. 36 Pressure measured at the flex pipe of the vehicle circuit downstream pressure regulator to the rail through different cross section of pipe

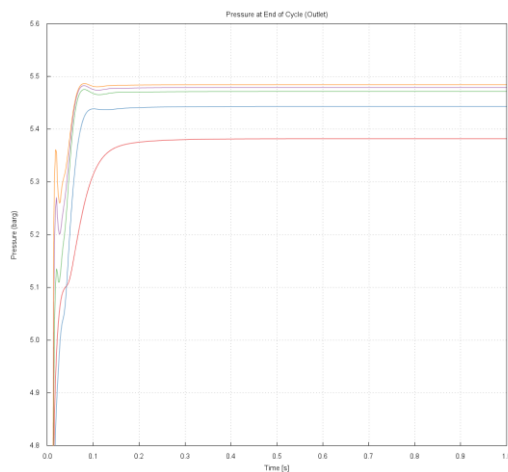


Fig.3. 37 Magnified section of pressure measurement in the flexpipe

Rail:

The pressure regulator in the LNG circuit was designed to set pressure of 6 barg , thus the gas which are higher than set pressure limit was reduced and when the pressure limits upstream are equal to or lower than the set limit the regulator becomes permeable, here in our case all the input pressures are more than the set limit , thus we can observe the pressure was limited,

Thus all the output from the downstream of the pressure regulator should be equal to the set limit, thus we directly measure the pressure in the rail, the variation in the pressure difference was observed in the graph since the cross section case study was incorporated down stream

the pressure regulator too, thus we pressure loss various from regulator part to the rail section.

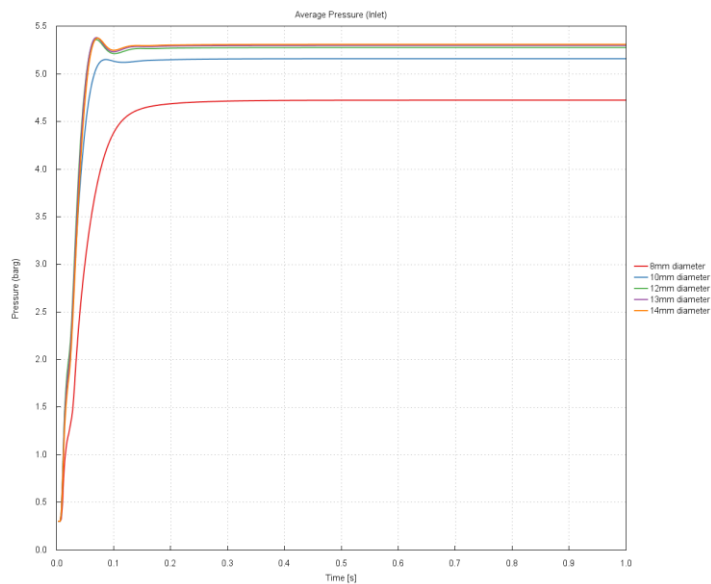


Fig.3. 38 Pressure measured at the rail of the vehicle circuit cross section of pipe

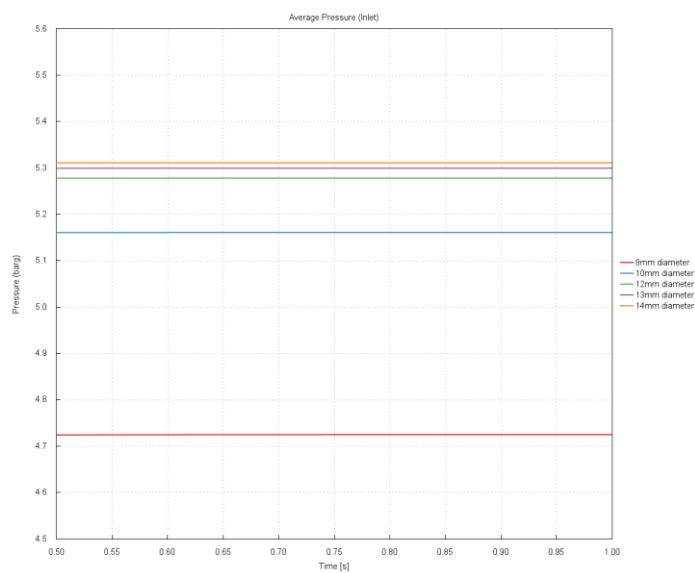


Fig.3. 39 Magnified section of pressure measurement in the rail

3.6.1 Vehicle simulation conclusions

Connecting tube from Regulator to Engine in test bench:

From the simulation results from the CNG and the LNG circuit , the behaviour of the two system down stream the pressure regualtor behaves the same. The fuel which was stored in different form reaches the same state and identical condition downstream the pressure regualtor, from the extensive analysis the pressure upstream the regulator has suffient pressure to keep the downstream pressure constant.

It was observed at the both cases the pressure loss was found extensively high in the conneting tube upstream the rail compared to other parts in the circuit, thus we developed a complete model of the connecting tube which was used in the vehicle and developed a dash board.

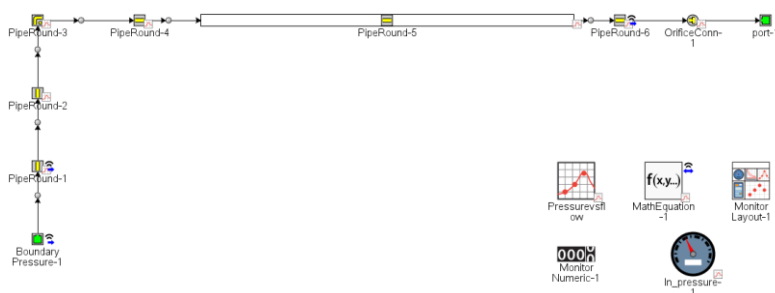


Fig.3. 42 1D model of the connecting tube from regulator to rail

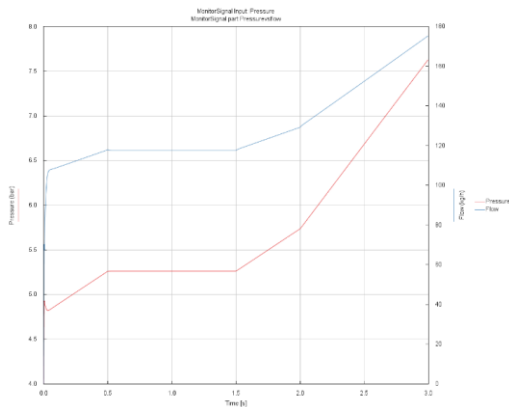


Fig.3. 41 Transient input pressure given to the circuit and measured mass flow rate (case 1)

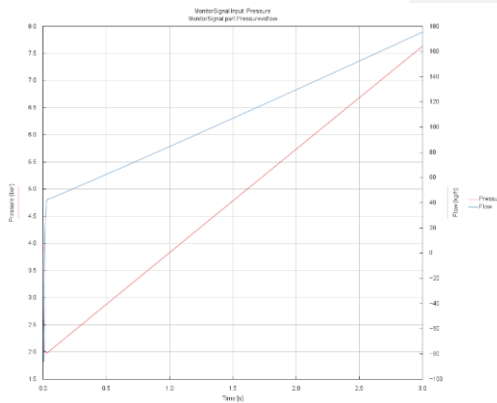


Fig.3. 40 Incremental pressure given to the circuit and measured mass flow rate (case 2)

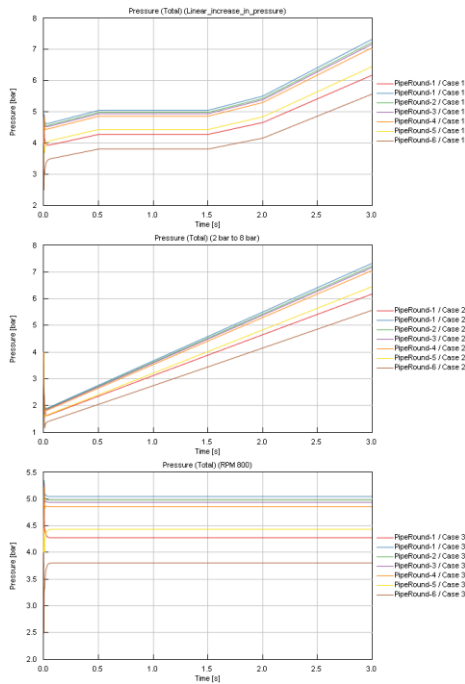


Fig.3. 43 Pressure measured at all the pipes in the circuit

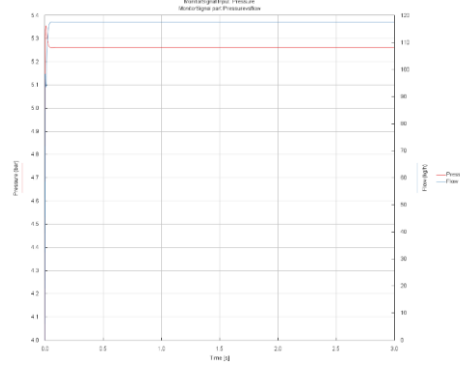


Fig.3. 43 Constant input pressure given to the circuit and measured mass flow rate (case 3)

Thus, from the following simulation data from the three input pressure, we obtained an optimum pressure loss at each part of the tube and the total pressure loss was calculated. This measured loss was matching with the results from the vehicle data where the pressure loss in range of 1.5-2.0 bar

Components	Pressure drop (barg)
Piperound-1	0.148
Piperound-2	0.076
Piperound-3	0.170
Piperound-4	0.061
Piperound-5	0.745
Piperound-6	0.728
Total pressure loss	1.92 barg

The completion of the thesis work represents a significant achievement in the development and application of a model originally designed for a laboratory test bench and subsequently extended to the vehicle model. This pathway involved a systematic approach that integrated experimental data from the engine test bed and allowed for the identification of pressure losses in the natural gas fuel lines due to flow and pressure oscillations. This successful extension of the model to the vehicle system represents a significant milestone in the study.

The subsequent phase included laboratory tests on a special test rig. These empirical tests provided important data for the validation of the recognition model. The model developed during this phase aimed to accurately identify pressure loss within the circuit. The laboratory tests not only served to validate the model, but also provided practical insights into the real-world performance of the circuit. The error measured was with close tolerance within the range of **5% error tolerance**

Once the detection model was successfully validated, the study moved on to applying this model to measure the pressure loss within the vehicle circuit, considering a range of operating parameters such as pressure, load and temperature, the effectiveness of the model in detecting pressure loss under different conditions was investigated.

The correlation between the model-derived pressure drop values and practical measurements on the vehicle's rails was critical in supporting the validity and effectiveness of the developed model. This validation is indicative of the successful translation of theoretical concepts into practical scenarios. The model's ability to accurately predict and determine pressure drop, confirmed by correlation with actual measurements, underscores its credibility and reliability in evaluating the performance of natural gas cycles in heavy-duty truck engines.

3.7.1 Extension:

Beyond the pressure loss model development, the dashboard which was produced during the steps was a mile stone in the project. This dashboard was virtually replicating the complex software which test the same data, but once we have the experimental data of certain points this simulation tool can replace the human efforts and hard labor on the test bench, it was easy to predict and calculate by running the simulation, thus the 1D simulation gave the edge over solving complex simulation in CFD software's which takes huge time, this mathematical model was close enough to understand the problems and can be fix faster compared to conventional CFD tools available.

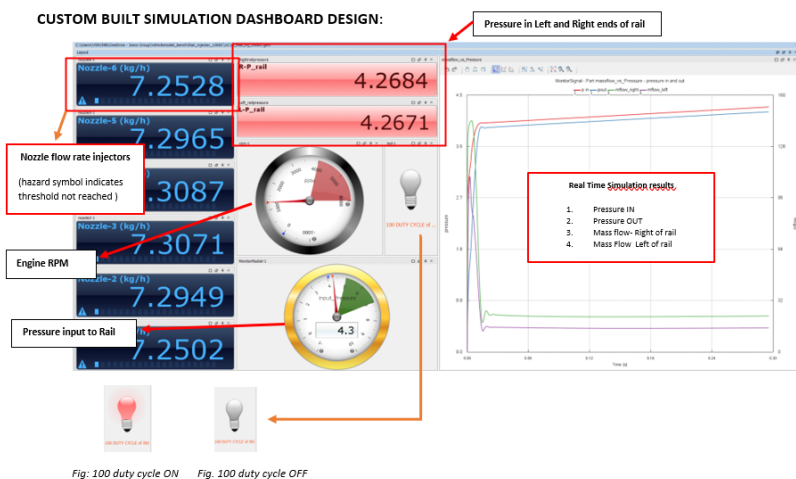


Fig.3. 44 dashboard developed for rail to measure injector mass flow and flow quantity while simulation

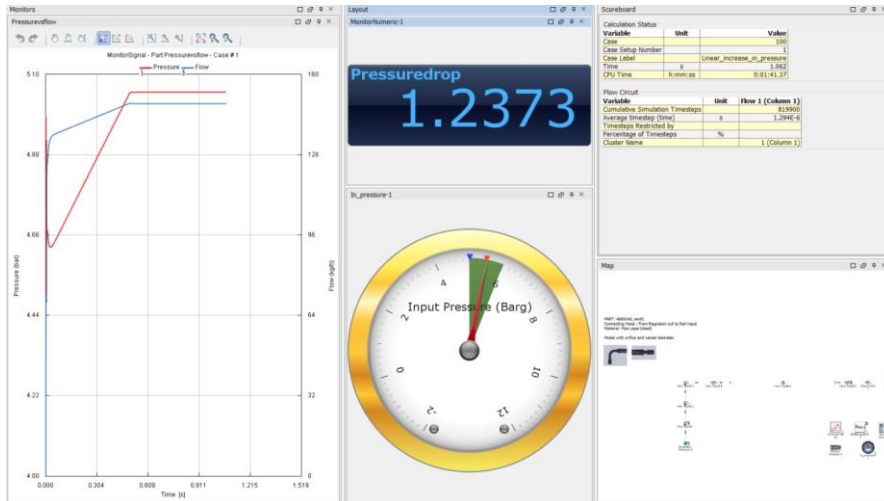


Fig.3. 45 Dash board designed for connecting pipe from regulator to rail to verify flow and pressure loss during runtime

4.Conclusion

The conclusion of this work is based on the confidence that the developed model is a robust and reliable tool for determining natural gas circuit pressure losses which was validated by correlations between the model's estimates and experimental measurements, provides a basis for optimizing the design and operation of these circuits in heavy-duty truck engines. Ultimately, this work not only contributes to the advancement of green transportation technology but also represents a significant step toward improving the efficiency and environmental performance of heavy-duty truck engines that use natural gas and bio-Methane as an alternative fuel source.

BIBLIOGRAPHY AND SOURCES